BAA British Astronomical Association

Mercury Observing Guide

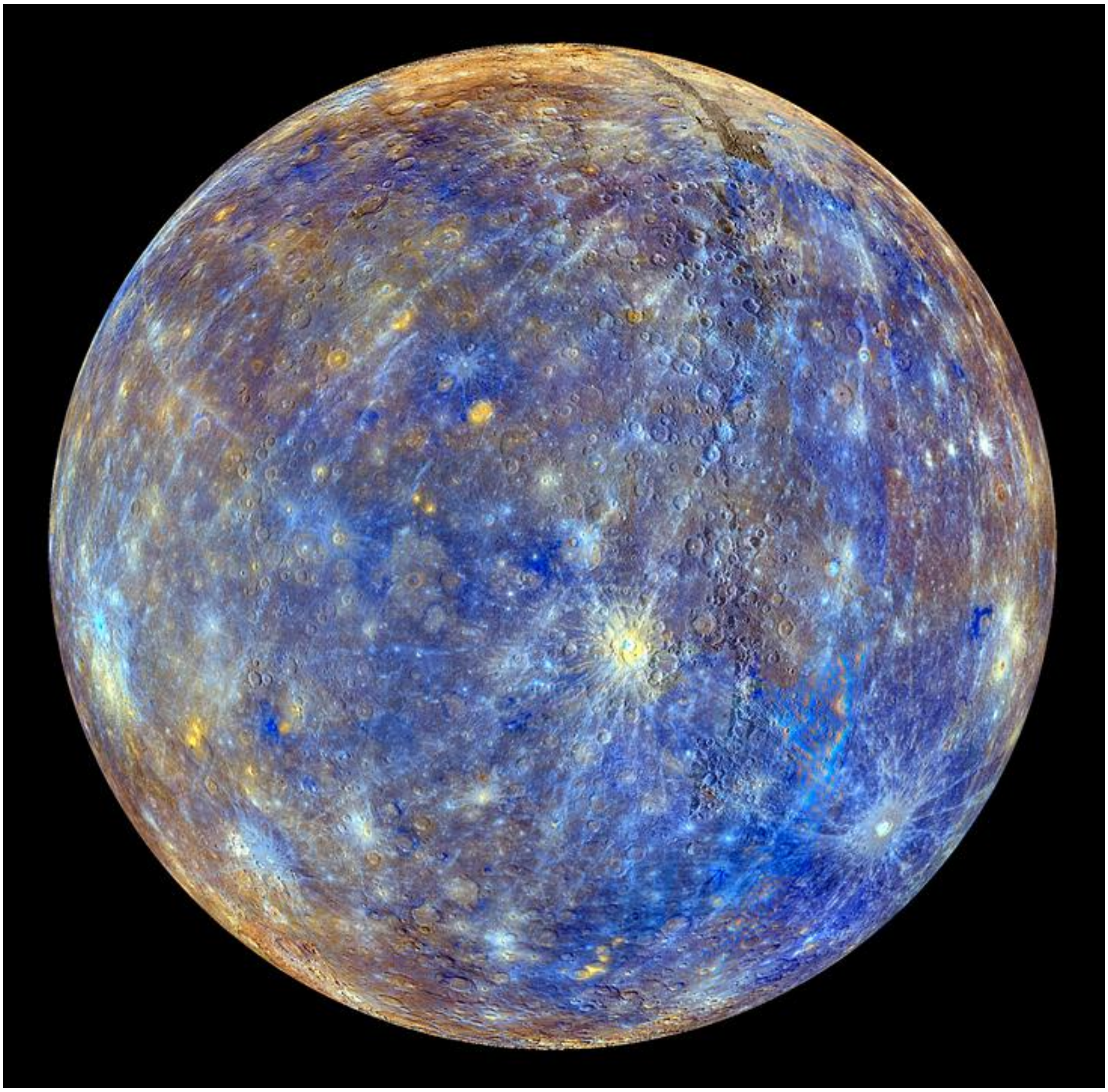

Chris Hooker

Mercury Observing Guide

Second Edition

Chris Hooker

Mercury Coordinator, Mercury and Venus Section

Cover image: colour-enhanced view of Mercury obtained by NASA's Messenger probe

Credit: NASA / Johns Hopkins University Applied Physics Laboratory

Contents

Preface to the Second Edition

This is the second edition of the BAA Mercury Observing Guide which was first published in 2020. The popularity and usefulness of guides such as this is hard to judge, but one measure is the number of copies sold at exhibitions and other events where the BAA has a presence. In 2024 the BAA sales co-ordinator arranged for a second print run to ensure there would be enough copies available for some years to come, so clearly there is a demand for the Guide from both BAA members and members of the public who attend these events.

This edition is not greatly changed from the first. Nothing has been removed, but it contains an extended section about imaging Mercury's sodium tail, which was described only briefly in the previous edition. The Gallery section has been updated and extended with images obtained over the last five years, including some of the elusive sodium tail. There is a new Appendix describing the design and construction of a parfocal Barlow lens that works better for infra-red imaging of Mercury (and other targets) than regular visual Barlows. The writer also took the opportunity to edit the text in a few places to improve clarity and to correct a few errors that escaped detection during the proof-reading of the first edition.

This edition will not be available in printed form for some time, but BAA members can access or download it from the web page of the BAA Mercury and Venus Section.

Chris Hooker, October 2025

1. Introduction

Mercury, the innermost planet of the Solar System, receives relatively little attention from amateur astronomers. Reasons for this may include the greater attraction of the showpiece planets Venus, Mars, Jupiter and Saturn, the perceived danger of observing Mercury, the restricted periods when the planet can be seen and a belief that no useful observations can be made. Indeed, the Messenger probe returned a wealth of information about Mercury that no terrestrial observations can hope to match, and there is no question that Mercury offers a significant challenge to observers who want to do more than simply see it in the twilight sky. All these factors aside, there will still be some whose goal is to observe the planet and try to pick out features on its surface. This guide is intended to be a collection of useful information and techniques to help and encourage anyone who wants to observe Mercury at any level.

One reason why Mercury should be observed is simply the fact that relatively few observers do so, thus the value of a good observation is increased by its rarity. Another reason is that very few bodies in the Solar System show a solid surface on which detail can be seen. Of those that do, Mercury is third in order of apparent size after the Moon and Mars, and the next largest are Ganymede and the other Galilean moons of Jupiter. Careful observation or imaging of Mercury can thus reveal permanent markings that few will have seen before.

Some of the reasons listed above for not observing Mercury have become less significant in recent years thanks to developments in the equipment available to amateurs. The dangers that were highlighted prominently in past advice can be reduced or avoided by the correct choice of telescope and mounting, and the use of automation. Nevertheless, safety must always be a prime consideration when locating and observing Mercury, and it is discussed in detail in Section 2 of this guide, as well as in other places where it is relevant. The take-away message is that although techniques exist to observe Mercury safely at most times, if observers do not feel comfortable using those techniques, they should not attempt the observations. There are many other objects in the skies.

My first attempts at webcam imaging of Mercury were in May 2006, using a 10-inch Newtonian and a Philips ToUcam. At the start, simply locating Mercury was a challenge, and my early images showed only the phase and occasionally some poorly-defined bright patches. The learning curve to achieving good-quality images was steep, but the results improved with experience and the development of new methods, some of which are described in this guide. However, after a few years, I felt that I was making no further progress, and I moved on to other subjects. It was only in 2017, when the major planets had all moved into the southern sky, that I decided to start imaging Mercury again. With the benefit of far more experience and better equipment, the results were also far better. I regularly obtained images showing albedo features that agreed with maps from spacecraft data, and many of these can be found on my page in the members' section of the BAA website. In 2019, at the invitation of Paul Abel, the new Director of the BAA Mercury and Venus Section, I became Mercury coordinator for the Section. It was Paul's suggestion that I should write a guide to observing Mercury, to pass on my experience and encourage the observation of this little-known planet.

My aim has been to bring together techniques for locating, observing and imaging Mercury safely and effectively, so that would-be observers can find and observe the planet with confidence, and do so more often. Lists of references and links to supporting material are given to stimulate interest and to provide background information. I hope this guide will encourage more amateurs to observe Mercury, and thereby contribute in a small way to our understanding and appreciation of this little world.

Chris Hooker, April 2020

2. Safety in observing Mercury

2.1 Safety and risk assessment

Modern principles of safety management emphasise the importance of risk assessment when carrying out potentially hazardous activities. The essence of this is simply to think carefully, in advance, about what the hazards of the activity are, what kinds of harm they could cause, how severe that harm might be and how likely it is to occur. Once the risks are properly understood, ways can be found to either avoid them entirely, or minimise them by reducing their severity and likelihood. This section of the guide discusses the risks of locating and observing Mercury, and how those risks can be reduced to an acceptably low level. However, what one person finds acceptable may not be so for another, and a few of the techniques discussed in later sections may be seen by some as unacceptably risky. Before observing, it is worth making a checklist of the steps to be performed, including safety checks, which can be followed when at the telescope. The writer recommends that all observers of Mercury do this, and adopt the cautious approach of asking themselves, before carrying out each step from the list, “Is the risk of doing this acceptable?”. Using this approach will allow you to observe Mercury without injuring yourself or damaging your equipment. Remember that a risk assessment is specific to the circumstances, so do not use the information in this guide as a substitute for doing your own.

2.2 Hazards

Mercury never appears more than 28 degrees from the Sun, and this proximity is what gives rise to the danger associated with looking for and observing it, because the planet cannot be seen through a solar filter. Using any kind of unfiltered optical aid to search for Mercury when the Sun is above the horizon exposes the observer to the risk of direct sunlight being collected and concentrated on the eye. This would result in severe damage to the retina and cause immediate and permanent blindness in the affected eye. The greatest risk lies in the use of binoculars, because they are usually hand-held and free to move, rather than being supported on a fixed mounting, have a wider field of view than a telescope and because both eyes would be damaged if the Sun were to be viewed accidentally.

The safest rule is NEVER USE BINOCULARS TO LOOK FOR MERCURY IN DAYTIME.

Every precaution must be taken to avoid accidental viewing of the Sun through an unfiltered telescope. By using the correct techniques, however, it is possible to locate and observe Mercury safely, even in daytime. The advice never to sweep the sky near the Sun with an unfiltered telescope is absolutely sound, but was written at a time when the mountings owned by amateurs were typically either altazimuth types or basic equatorials equipped only with setting circles. Furthermore, obtaining a position for Mercury that was sufficiently accurate to locate it was not the trivial task it is today, with the availability of planetarium programs and online ephemerides. Positional tables such as the BAA Handbook do not give positions for every day, so observers had to interpolate to the time when they wished to observe. Even starting from the Sun (with a solar filter on the telescope) and making the most accurate offset possible using setting circles, it would be necessary to scan around the expected position after the filter had been removed. A momentary lapse of attention by the observer during this process could result in the Sun entering the field of view, with very serious consequences. Modern automated mountings eliminate the need for uncontrolled sweeping, and allow Mercury to be found easily and with minimal risk.

2.3 Light-baffles for observing and imaging Mercury safely

Mercury can be observed in complete safety by ensuring that no sunlight strikes the objective or mirror of the telescope. There is then no image of the Sun or any concentration of sunlight by the optics. When the telescope is aimed at Mercury, assuming it is firmly mounted and properly driven, there is no reason why it should move unexpectedly so that the Sun enters the field of view. A suitable light-baffle attached to the telescope tube will screen off the sunlight when the instrument is aimed far enough from the Sun, and the minimum safe angular separation between the Sun and Mercury can be calculated using simple trigonometry, as shown in Figure 1, below. In the examples shown, for a refractor and a Newtonian, the telescope is assumed to be aimed at Mercury, and the minimum safe separation angle θ between the Sun and Mercury is given by the expression

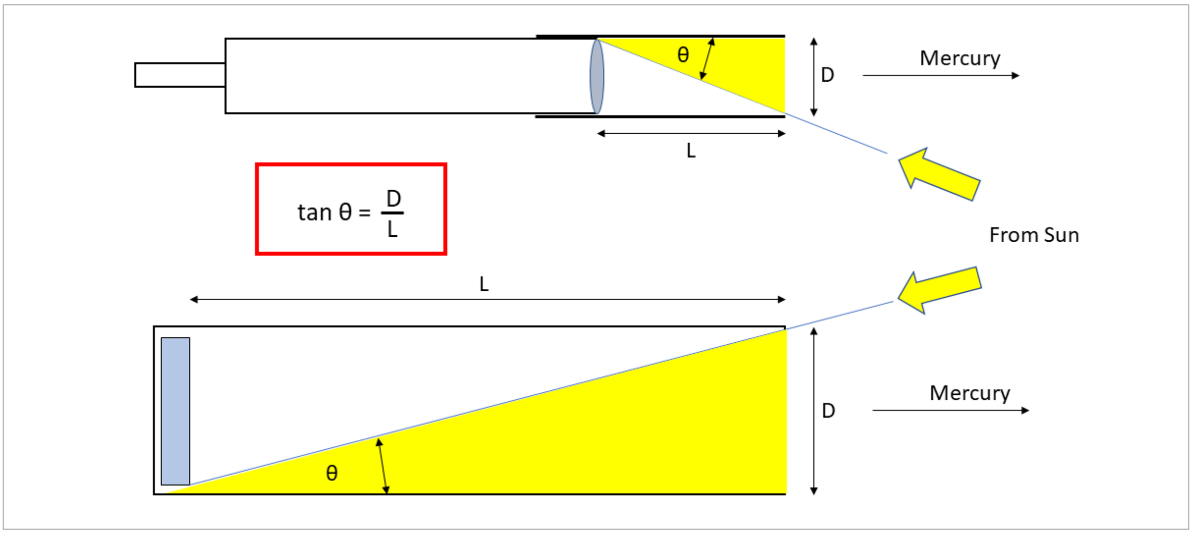

Figure 1. Examples of a light baffle (on a refractor) and a solid-tube Newtonian telescope, showing the minimum angular separation θ of Mercury from the Sun for safe observation.

$$\tan \theta = D / L \tag{1}$$

where D is the diameter of the light baffle or the telescope tube, and L is the distance between the open end of the baffle and the objective or primary mirror of the telescope. In the case of a Newtonian with a solid tube, the tube itself serves as the light-baffle, and the minimum angle can be calculated in the same way. For a Schmidt-Cassegrain (SCT) or a Maksutov, the distance L must be measured from the front of the light-baffle to the mirror, rather than the corrector plate, because the corrector does not focus the light to a significant degree. However, those types of instrument usually have primary mirrors with short focal ratios, and for them the minimum safe angular distance of Mercury from the Sun will be greater, or the light-baffle longer, to ensure that no sunlight enters the instrument. Figure 2 shows graphically

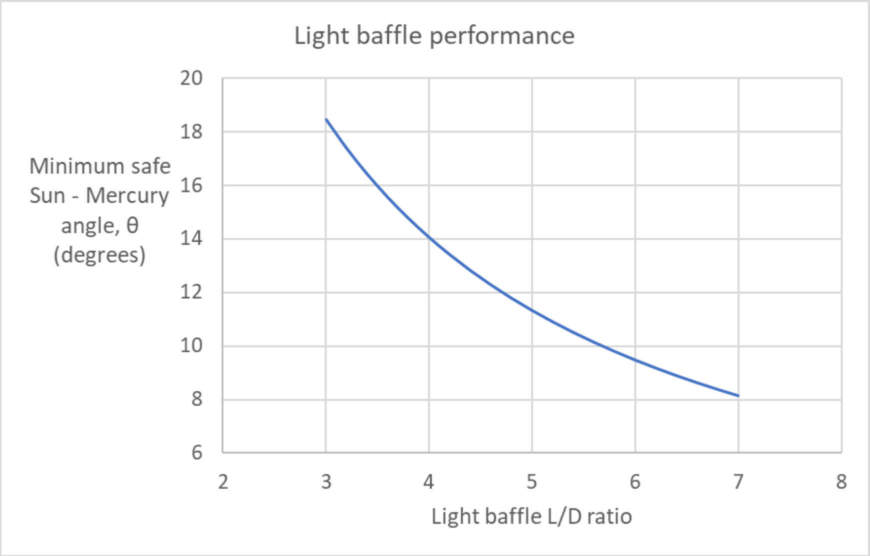

Figure 2. Graphical representation of Equation (1), showing how the minimum safe angle between the Sun and Mercury varies with the light-baffle dimensions.

how the minimum value of θ varies with the L/D ratio of the baffle, for values of L/D that are likely to be useful in practice. You should know the minimum safe angle for your instrument, and bear this in mind when deciding whether or not to observe after finding the elongation of Mercury in the procedure described in Section 4.3. Using a telescope with a light-baffle having L/D = 5, for example, will allow Mercury to be observed safely any time it is more than eleven degrees from the Sun. In practical terms, this corresponds to at least half of each elongation, although the exact period will vary depending on how far Mercury moves from the Sun. Most importantly, using a light-baffle will allow observations to be made in daytime when the planet is well above the horizon.

2.4 Specific requirements for a light-baffle

An external light-baffle similar to the one described above will be needed for the tube of a refractor, SCT or Maksutov if the instrument is to be used for observing Mercury in daytime. The length of the baffle will depend on the aperture and the minimum separation of Mercury from the Sun at which it is desired to observe. It is worth noting that the short dew-shield often supplied with a small refractor is rarely long enough to be an adequate light-baffle, but can be used to support a home-made one. The baffle needs to be light, rigid and opaque, and must have a means for attaching it firmly to the tube of the telescope. When used with the baffle, the telescope may need to be rebalanced, and the extended length of tube will act as a very effective sail, catching the slightest breeze and causing the telescope to move or shake. It is also important to ensure the baffle is held firmly so it cannot slide down the tube of the telescope, as this would reduce the effective length L, and render the baffle unsafe at a time when it was theoretically safe to use.

Figure 3. Example of a light-baffle. Chris Dole's 180 mm Maksutov (left panel) with the normal dew-shield/light baffle (middle panel) and the temporary extended light-baffle (right-hand panel).

Figure 3 shows a home-made dew-shield and light-baffle for a SkyWatcher SkyMax 180 mm Maksutov-Cassegrain telescope owned by Chris Dole, who frequently images Venus and Mercury. The primary shield is made from “a stiff, felt-like material” which, like the main tube of the telescope, is covered with aluminized Mylar to reflect the heat. It is fixed to the casting at the outer end of the tube which holds the correcting lens. The L/D ratio for the primary shield is about 4.8, allowing imaging up to 12 degrees from the Sun. To reach Mercury or Venus when they are closer to the Sun, he attaches a temporary extension screen, shown in the right-hand image, which increases the L/D to 6.6. The cardboard screen can be rotated around the tube axis so it is correctly placed to screen off the sunlight.

It is essential that the light-baffle can be fitted with a full-aperture solar filter, if the Sun is to be used as a reference point for locating Mercury. The method described in Section 4 depends on aiming the filtered telescope at the Sun, which is the only astronomical reference point consistently available in daytime, then moving the telescope to the expected position of Mercury. After the filter is removed, the light-baffle still needs to be in place to ensure no sunlight is collected by the telescope optics. Each observer must ensure that their solar filter can be attached securely to the light-baffle, and removed when looking for the planet. The writer recommends using a Newtonian with a solid tube for observing Mercury, as the light-baffle is simply the telescope tube, and the filter can be mounted securely on the front of it. If a home-made light-baffle is used for a refractor, SCT or Maksutov, the method of attaching the solar filter to the end of the baffle must be carefully thought out to ensure it cannot fall off. The requirement is exactly the same as for observing the Sun itself. One option would be to incorporate the filter into a sleeve that slides over the end of the baffle, and can be held in place by some positive means.

It is worth noting that even when sunlight does not hit the optics of the telescope, it still strikes the inside of the light baffle, or the tube in the case of a Newtonian. This will result in localised warming which may cause convection currents, disturbing the air and reducing the stability of the image. In practice, the seeing during daytime is likely to be relatively poor compared to night-time observing conditions, so the effect of the additional heating will be less noticeable.

2.5 Alternatives to light-baffles

If the observer is fortunate enough to have an observatory, then it may not be necessary to attach a light-baffle to the telescope itself, if some part of the observatory dome, or its roof, can be used instead to screen the instrument from the Sun. Another possibility is to use a sun-shield mounted on a pole or supported on the observatory roof. The safety requirement is met provided the telescope aperture is in the shadow of whatever screen is being used, but the position of the screen will need to be changed from time to time as the Sun moves west. Placing a (portable) telescope in the shade of a building can also be effective, but this technique is subject to the same time restrictions as twilight observing. After a while the Sun will emerge or Mercury will disappear behind the building, at which point either the telescope will have to be moved and the planet re-acquired, or the observing session ended. The major disadvantage of using a building to block the sunlight is that the Sun cannot be used as a reference point for locating Mercury.

3. Visibility of Mercury

3.1 Naked-eye viewing of Mercury

Mercury's orbital inclination relative to the plane of the ecliptic is 7 degrees, larger than any other planet. Its orbit is also more eccentric than any of the other planets, so that its distance from the Sun varies from a maximum of 0.47 AU to a minimum of 0.31 AU. Taken together, these factors result in large variations in both the greatest elongation of Mercury from the Sun, ranging from eighteen to twenty-eight degrees, and its altitude at any given location. The planet can only be seen with the naked eye in twilight, and as a general rule for observers in the northern hemisphere, Mercury is at its greatest altitude in the evenings at eastern elongations around mid-March, and in the mornings at western elongations around mid-September. In the southern hemisphere, the best times are western elongations on March mornings, and eastern elongations on September evenings. Of course, the planet can also be seen at other times, and its location and altitude are easily found from tables or by using one of the many available planetarium apps. For those who merely wish to see the planet in the twilight, the information above will be sufficient. The remainder of this section considers the geometry of Mercury's orbit in more detail, and how it affects the visibility and when observations can be made.

3.2 Mercury's orbital geometry

Figure 4 shows the orbits of Mercury and the Earth to scale, from a viewpoint to the north of the ecliptic, so that both planets appear to orbit anticlockwise. Mercury's orbit is visibly elliptical, and the part of it that lies south of the ecliptic is shaded grey. The semi-major axis of the orbit and the line of nodes are shown. Longitudes of significant points are marked, and alternate calendar months are labelled and indicated by blue shading around the Earth's orbit: these refer to the Earth's position.

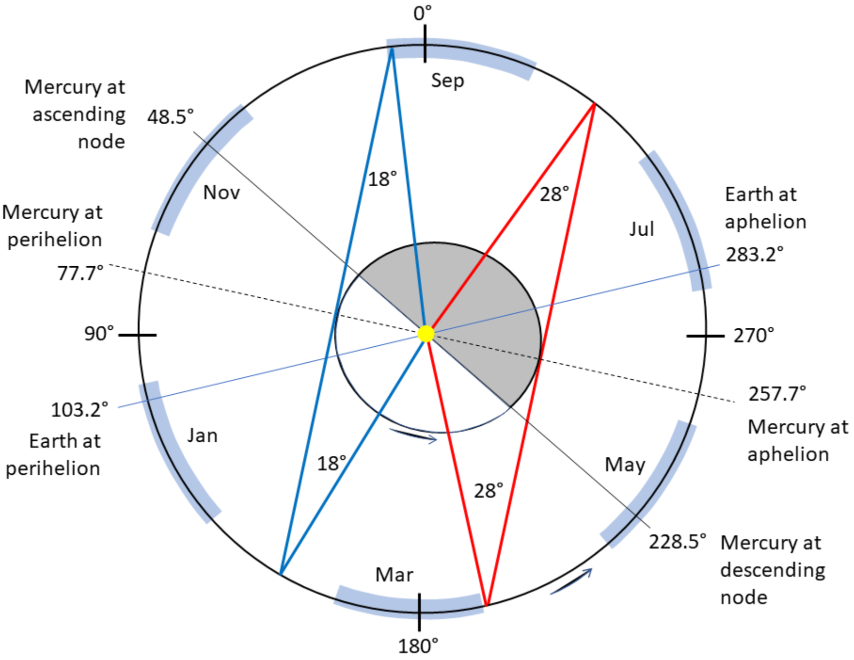

Figure 4. Diagram showing the orbits of Earth and Mercury, the longitudes of significant points, and the occurrences of maximum and minimum elongations of Mercury.

The orientation of the semi-major axis of Mercury's orbit lies along longitudes 78 degrees to 258 degrees, and the times at which the planet's elongation from the Sun is greatest occur when Mercury is at aphelion and the Earth is at one of the points on its orbit where the line of sight to Mercury is perpendicular to the semi-major axis. These points occur in early April and mid-August, at which times the elongation of Mercury can reach its maximum value of 28 degrees. This is shown by the red lines in Figure 3. At those times, Mercury is slightly south of the ecliptic. The smallest value of the maximum elongation angle is 18 degrees, which occurs in either mid-February or late September, as shown by the blue lines in Figure 3, and at those times the planet is slightly north of the ecliptic.

However, the times of greatest elongation are not necessarily those at which the planet is most visible. There is another factor to consider, which is the orientation of the ecliptic relative to the observer's horizon. For northern hemisphere observers, the time of greatest visibility during eastern elongations is near the spring equinox in March, when the ecliptic is steeply inclined to the horizon in the evenings. For western elongations, the time near the autumn equinox in September is when the ecliptic rises steeply above the horizon, so Mercury will be highest in the sky before dawn. Similar arguments apply in the southern hemisphere, where western elongations in March and eastern elongations in September provide the best opportunities for observing the planet when it is well away from the horizon. It is worth spending some time with a planetarium program such as *Stellarium* to become familiar with the way Mercury's visibility changes from your location.

3.3 Transits of Mercury

Because Mercury orbits between the Sun and the Earth, it is possible for it to pass directly between Earth and Sun in an event known as a transit. There are two requirements for this to happen. Firstly, Mercury must be at inferior conjunction, in other words at the point of its orbit where it is directly between the Earth and the Sun as seen from above or below the ecliptic. Mercury's orbit is inclined at 7 degrees to the plane of the ecliptic, which means that at most inferior conjunctions the planet will appear to pass north or south of the Sun. The second requirement for a transit is that the Earth is close to the line of nodes of Mercury's orbit, where the orbital planes of the Earth and Mercury intersect, so that Mercury's orbital path appears to cross the Sun's disc. The Earth passes through the line of nodes in early May (the descending node) and early November (the ascending node). Transits of Mercury occur only around those dates. In a similar way, solar eclipses occur only when the Moon is new and the Earth is close to a node of the Moon's orbit, so the orbit of the Moon appears to cross the face of the Sun.

The longitude of Mercury's ascending node is 48.52 degrees, compared with the longitude of its perihelion which is 77.71 degrees. Mercury reaches perihelion shortly after passing its ascending node, and this means that the planet appears slightly smaller against the Sun during November transits than it does at May transits, when it is near aphelion and thus closer to the Earth. Transits in May are about half as frequent than those in November, because Mercury's greater distance from the Sun in May, and correspondingly lower orbital velocity, means there is a smaller probability of the planet being at inferior conjunction during the time the Earth is close to the node. However, a May transit can last for nearly eight hours if Mercury passes centrally across the Sun, compared to a maximum of five and a half hours for a November transit. In the case of a central transit, some part of the event will typically be visible from approximately three-quarters of the Earth.

For northern hemisphere observers, the weather is likely to be more favourable in May than in November, and the Sun will be higher in the sky, making May transits perhaps easier to observe. In the southern hemisphere, November transits are in general more favourable. The dates of the ten remaining transits in the 21st century are as follows, with the part visible to UK observers indicated:

Nov 13, 2032 [End]; Nov 7, 2039 [End]; May 7, 2049 [All]; Nov 9, 2052 [None]; May 10, 2062 [Start]; Nov 11, 2065 [None]; Nov 14, 2078 [All]; Nov 7, 2085 [All]; May 8, 2095 [Start]; Nov 10, 2098 [End].

4. Finding and observing Mercury

4.1 Twilight observations

The discussion in Section 3 about the visibility of Mercury relates to spotting the planet with the naked eye. The difficulty and risk of locating Mercury in daytime was the main reason for the advice, given in older texts, that Mercury should be observed through a telescope, and especially through binoculars, only in twilight when the Sun was below the horizon. Observing at those times eliminates the risk of damage to the eyes, but of course Mercury itself is fairly close to the horizon, and the advice is in sharp contrast with the usual recommendation to observe astronomical objects when they are as high in the sky as possible. At twilight the observer is looking at Mercury through a greater thickness of atmosphere, with the result that the seeing, extinction and atmospheric dispersion combine to give a relatively poor view at best. Furthermore, the time available for observation before either the Sun rises or the planet sets is often rather short. Observers at coastal sites may be able to take advantage of the steadier seeing offered by a sea horizon, but for the majority it is likely that observing Mercury at such restricted times would be a frustrating experience. It is better to observe or image Mercury when it is higher in the sky and the degrading effects of the atmosphere are significantly reduced. The problem then is to locate the relatively faint planet in a bright sky close to the Sun, and we need to consider how this can be achieved in safety.

4.2 Finding Mercury with a computerized mounting

It is clear that the risks described in Section 2 are mostly associated with finding Mercury rather than with observing it once found. The availability of modern computer-controlled mountings with drives and encoders for position setting has changed the way in which amateur astronomers locate objects. By following the correct procedure, an observer can locate Mercury either without any sweeping, or with only a minimal amount of sweeping in a way that will never result in unfiltered sunlight reaching the eye or the camera. The best technique may vary depending on the exact type of mounting and telescope. A technique for observers using simpler types of mounting is described later in the section.

The writer recommends the following procedure: it assumes a polar-aligned equatorial mount with drives, encoders and a readout that gives RA and Dec positions. The principle is to use the Sun as a starting point, and to offset the telescope in each coordinate by the correct amount to find Mercury.

1. Use a planetarium program such as *Stellarium* to find the coordinates of the Sun and Mercury at the planned time of observation. Also note the planet's elongation from the Sun, and confirm that the elongation is large enough for safe observation with *your* telescope (see Section 2.2).

2. Work out the offsets in RA and Declination required to move from the Sun to Mercury.

3. Attach full-aperture solar filters firmly to the main telescope and all finders.

4. Aim the telescope at the Sun and focus carefully: on a sunspot, the solar granulation or the Sun's limb. It will be very hard to locate Mercury if it is out of focus. Use an eyepiece that allows the whole solar disc to be seen. It is highly desirable to have a crosshair or similar feature in the focal plane.

5. Centre the telescope on the Sun's disc, and note down the coordinates from the readout.

6. Using the offset values found in step 2, calculate the expected position of Mercury. Alternatively, if your mount allows it, set the coordinates to those found for the Sun in step 1.

7. Drive the mount to the predicted position of Mercury, and remove the solar filter (from the main telescope only).

8. Confirm visually that no sunlight is hitting the telescope objective or mirror.

9. Look through the eyepiece and try to locate Mercury.

While looking for Mercury through the eyepiece you will probably find it difficult to keep your other eye open. At night you can usually do that and ignore what you see with the non-observing eye, but in daylight this is nearly impossible, so you will have to close the other eye, or wear an eye-patch. However, either of these can result in the eyes relaxing so their focus changes, and the planet will then be very hard to see. The best solution is to use an eyepiece with a crosshair or some other feature in the focal plane. The eye will naturally focus on this, so if you use the same eyepiece throughout the process, Mercury will be in focus in the field of view.

Whether Mercury is visible immediately depends on how well the mount is polar-aligned and how accurately the coordinates were determined. If you have a permanent mount in an observatory, the alignment should not be an issue, but for non-permanent setups it is best to align the mount on Polaris the night before, if possible. Spotting Mercury becomes easier with experience, but detecting the tiny pale speck of light in a featureless blue sky can be difficult the first few times. Slightly shaking the telescope can be helpful, as can driving the mount slowly north and south in Declination. Concentrate on the crosshair, and the movement of the planet in the field will often bring it to your attention. It may be worth fitting an orange or red filter to the eyepiece, to darken the sky and improve the contrast of the planet: note that adding the filter may change the focus. If Mercury does not appear after repeating the declination scan a few times, shift the telescope in RA by about half the field of view (say one quarter of a degree) in one direction and try again, then if necessary move in the opposite direction and do the same. It is good practice to confirm after each adjustment in RA that the light-baffle is still preventing sunlight from entering the telescope. If the sky is free of haze and high cloud, it should be possible to find Mercury when it is as faint as magnitude +0.5, corresponding to a phase a little less than 50%. Skies in the UK are rarely transparent enough to find it when fainter than this.

If Mercury remains elusive despite thorough searching, the only option is to replace the solar filter, move the telescope back to the Sun and try again. Check the coordinates carefully, and recalculate the offsets that are required. It is all too easy to make mistakes, particularly in the Declination offset if the Sun is on one side of the celestial equator and Mercury is on the other. Check the focusing again, in case the drawtube or the eyepiece shifted while the telescope was being slewed. In the writer's experience, the most common reason for failing to find Mercury is an error in the offset calculations, with poor polar alignment a close second.

4.3 Finding Mercury with non-GOTO mountings

If your telescope mount does not have position encoders and an electronic readout, but only setting circles, finding Mercury will be more difficult. The basic setting circles on many mounts are marked in steps of two degrees or more, so the accuracy of any offset from the Sun will not be good enough to put the planet in the field of view. It is fairly simple to construct a device to improve the accuracy of the RA offset, such as the one shown in Figure 5, which the writer used successfully for several years. It resembles a sundial, and was made from wood and a strip of stiff but slightly flexible metal. A nail at the front casts its shadow onto the scale, which was marked on graph paper and graduated in minutes of RA. The distance from the nail to the scale is 229 mm, so that I mm at the centre of the scale corresponds to 1 minute of RA, or 0.25 degree, and this is accurate enough for the purpose of locating Mercury. The device was held on the end of the declination axis of a GP-DX mount using the knurled screw that retains the counterweights. With the telescope aimed at the Sun, the device could be rotated around the axis so that the shadow of the nail fell on the scale, and the metal strip slightly twisted (if necessary) to centre the shadow on the zero point. The scale is marked on a flat surface, so the size of the divisions increases away from the centre. A cylindrical scale with its axis centred on the nail could have divisions of equal size, but would be harder to make.

Figure 5. The writer’s GP-DX mount showing the device used for offsetting in RA to locate Mercury. The telescope has been moved west so the shadow of the nail falls on the calculated point.

The procedure used with this device to locate Mercury was as follows. The calculated difference in RA between Mercury and the Sun was converted into minutes. To obtain the correct offset, the result was multiplied by the cosine of the *Sun’s* declination (the Sun being the reference point) because only on the equator is the angular size of one minute of RA equal to 15 arc minutes. The cosine factor adjusts for the way that meridians of RA converge away from the equator. The telescope was slewed to the predicted position in RA, so the shadow of the nail fell on the correct point of the scale, then the declination adjustment was made using the setting circle, and the solar filter removed. From this point the procedure was essentially the same as above, although some scanning in declination was usually required to locate the planet. Changes to the RA offset were made by either driving at double speed, or stopping the drive, for one minute, in order to move the field a quarter of a degree west or east.

A more sophisticated version of the alignment device could be made using a 2-dimensional scale and an opaque screen with a suitably-sized hole in place of the nail. This would throw a spot of light on the scale, which could then be used for both RA and Declination offsets.

5. Visual observations

5.1 Introduction

The term "visual observations" is used here to mean observing and drawing Mercury while looking at it through the telescope. This is of course the traditional method of observing, and before the development of photography and digital imaging it was the only means of recording the details seen on a planetary disc. In this digital age there are still some observers who continue the tradition, and although the writer is not one of them, this section is included for completeness, and to show what can be achieved by a skilled observer. The writer gratefully acknowledges the help and advice provided by David Gray, one of the few UK observers who currently observes and draws Mercury, from whom the following material is derived.

5.2 Choice of telescope

Any telescope can be used for observing Mercury in the twilight before sunrise or after sunset. The fortunate observer who has a choice of telescopes will select the one that best suits the circumstances of observation. Generally, the instrument with the largest aperture or the best-quality optics will be preferred, but if the instrument has to be moved to obtain an unobstructed horizon, portability of the telescope and mounting will become a factor. Mercury's small apparent diameter means that a relatively large magnification will be needed to pick out surface detail with any certainty, so telescopes of modest aperture, say 150 mm or less, will not give such good results. Regular observers and imagers of Mercury typically use apertures of 250 mm (10 inches) or more, in order to have enough resolution and light-grasp to sustain the necessary magnification. The optical type of the telescope is unimportant for twilight viewing, but this is not true in daytime. When the Sun is above the horizon, the optical design affects the safety of the instrument, and in particular the requirements for a light-baffle, as discussed in detail in Section 2.

5.3 Filters and other equipment

When observing Mercury in twilight, it is always at low altitude, and even if the seeing is good there will be atmospheric dispersion, which will spread the image into a short vertical spectrum. Given the small angular size of the planet, the dispersion can be a significant fraction of the image size. There are two techniques for dealing with this problem. One is to use a filter, either orange or red, which will both enhance the contrast of the albedo features and absorb the green and blue wavelengths which are the most highly dispersed. David Gray uses Wratten orange filters, No 21 or 22, for this purpose. Many different coloured glass filters are available, and the Wratten types have the number engraved on the outside of the filter mount.

As an alternative to filters, one of the commercially-available atmospheric dispersion correctors (ADCs) can be used. These reverse the dispersion of the atmosphere that spreads the light from the planet into a spectrum, and provide a clear view without the loss of light that occurs with a filter. The atmospheric dispersion varies with altitude so the ADC setting has to be adjusted from time to time, but this is usually straightforward. Mercury has little or no colour, so whichever technique is used, the view will be essentially monochrome.

Another piece of equipment that some planetary observers use is an apodizing filter. The aperture of a telescope is either a complete circle, in the case of a refractor, or an annulus for other types (Newtonians and Cassegrain variants) where there is a secondary mirror, usually circular, in the light path. The diffraction patterns produced by these two shapes are very similar, with a central bright spot and one or more diffraction rings surrounding it, as shown in the left-hand image of Figure 6. For an unobstructed aperture and a perfect optical system, the central spot, often known as the Airy disc, contains 84% of the light energy, and the remainder is distributed among the diffraction rings. When there is a central obstruction the shape of the diffraction pattern is almost the same, but the distribution of the light is different, with less reaching the central spot and more being thrown into the rings. The change only becomes noticeable to the eye when the diameter of the central obstruction is 30% or more of the aperture, but this is not unusual in Schmidt-Cassegrain instruments.

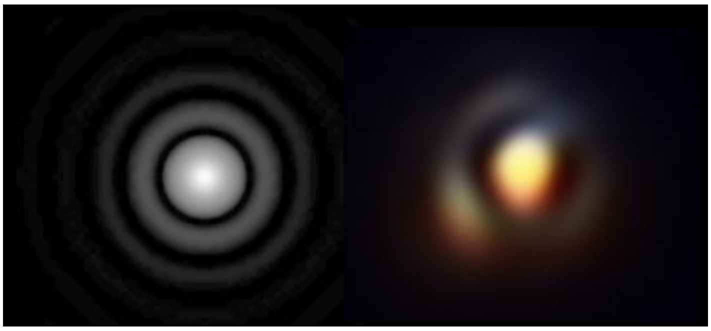

Figure 6. A schematic of the ideal appearance of the diffraction pattern at focus from a circular aperture, and a real star image, with atmospheric dispersion and parts of the first diffraction ring visible.

The diffraction pattern is generated by the hard edges of the telescope aperture. If the transmission of the aperture could be gradually and smoothly reduced towards the edge, the intensity of the diffraction rings would also be reduced, because the diffraction pattern of such an aperture resembles the Airy disc alone. This in turn would reduce the apparent blurring of the image due to diffraction. Making a telescope with such an aperture would be difficult, but the apodizing filter is a way to achieve something similar. A typical version, as used by David Gray, is an overlapped set of annular pieces of netting or mesh, such that there are three layers at the edge of the aperture, only two further in, then one and none towards the centre. Figure 7 shows an image of David's apodizer fitted to his telescope. He comments that the device works best in "mid-scale" seeing conditions:

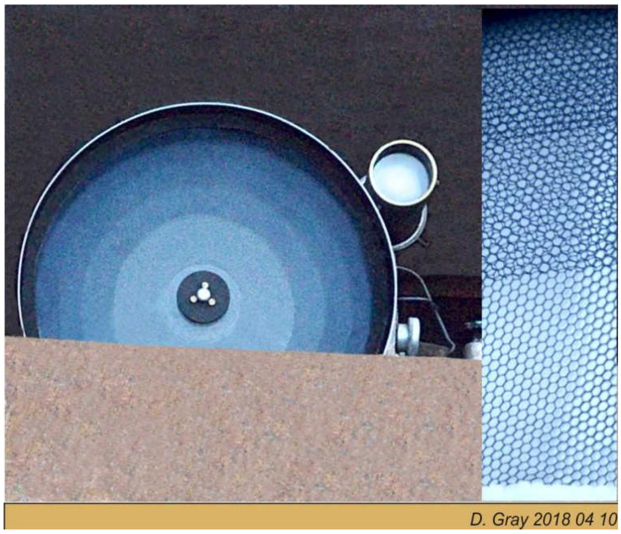

Figure 7. David Gray's apodizing filter fitted to his telescope, plus a close-up of part of it showing its structure.

". . . 'mid-scale seeing' being that where there is still a discernible/steadier central disk as with Pickering 4-7 but still some significant disturbance of the rings. In short: no clear (over-agitated) central disk, no real apodizing gain; and better than Pickering 7 little further improvement other than as a neutral filter." – David Gray.

The effect of the apodizer is to reduce the brightness of the Airy rings in the diffraction pattern. The rings are where most of the image disturbance occurs in those intermediate seeing conditions, so the result is to give sharper and clearer views with more detail. However, the visual field around the planet's image will no longer be 'clean' but will contain many diffraction artefacts produced by the screens. The observer must learn to ignore these and concentrate on the planet itself. Fred W. Price, author of *The Planet Observer's Handbook* (see Bibliography) also recommends using an apodizer.

5.4 Recommendations for visual observing

The following short list of notes and ideas has been drawn from various sources, in particular postings on the Cloudy Nights Forums by David Gray and others. Most of the information is in the form of brief comments in the text of the various sources, which is why the list-style presentation seemed appropriate.

1. Morning skies are often more settled. Sometimes shortly after sunrise there is a steadier interval before the seeing degrades again.
2. To see features visually requires very good conditions and plenty of experience of visual observing.
3. Higher magnifications, as much as 400x to 500x provided the conditions allow, make the difference between merely seeing features on the disc, and detecting structure within them.
4. The trick with Mercury in the mornings is to catch it in a darker sky and follow it until above (hopefully) the worst turbulence.
5. In colour Mercury appears in a darkened sky to be red or orange, but in a blue daylight sky it is very pale gray. Telescopic comparison in the same field of the telescope as Mars shows Mercury much less red than the ruddy planet.
6. “In good conditions the features on Mercury are not that difficult – contrary to the myths. Based on my impressions they might well look somewhat more contrasty than those of the moon if we could view them side by side at similar resolution.” – David Gray.

Patience appears to be essential for those wishing to see markings visually. A number of observers comment that they have had “a few” good sessions with the planet over a period of several years. It is clear, however, that good results can be obtained visually by a dedicated observer. Early observers of Mercury such as Schiaparelli, Flammarion and Schröter recommended observing the planet during daytime in order to avoid the atmospheric distortions that occur close to the horizon at twilight. Provided all necessary care is taken, as discussed in Section 2, this would appear to be good advice.

5.5 Recording visual observations

Records made of visual planetary observations usually take the form of a sketch of the planet, but this can be done in different ways depending on the observer’s preferences. The first method is to draw the outlines of distinct regions of different tone or colour on an outline blank showing the phase of the planet, and then label them according to the estimated tonal value on a scale from 1 to 10. A value of 1 is pure white and 10 is deep black: no texture can be seen in either of these values. Other areas are labelled from 2 to 9 according to the observer’s best estimate of the tonal value. An example of this type of record is shown in Figure 8, which was made by the Italian observer Gianluigi Adamoli. After completing a record of this type, the observer may choose to work it up into a pictorial representation of the planet, as Adamoli has done in this example. Others may prefer to simply draw the planet and any features as they

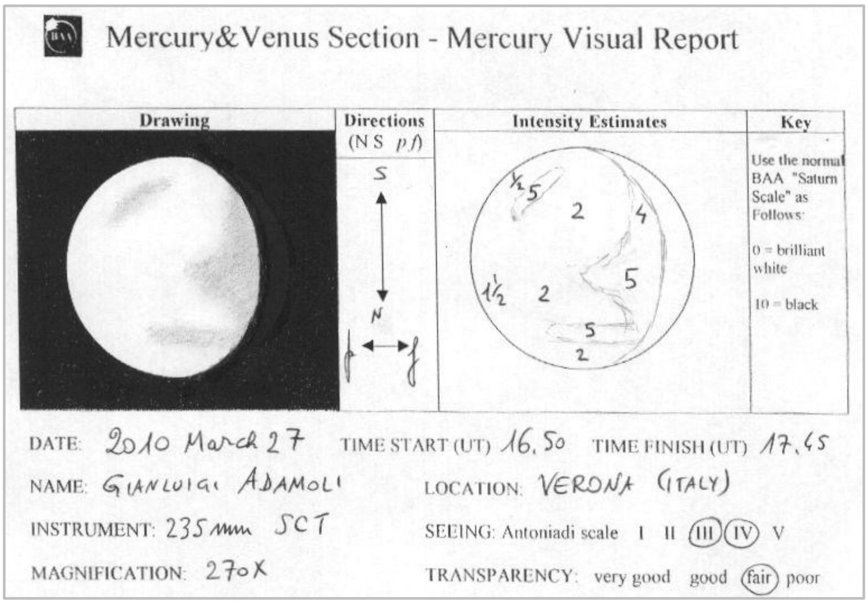
Mercury&Venus Section - Mercury Visual Report

Drawing	Directions (N S p f)	Intensity Estimates	Key
			Use the normal BAA "Saturn Scale" as Follows: 0 = brilliant white 10 = black

DATE: 2010 March 27 TIME START (UT) 16.50 TIME FINISH (UT) 17.45

NAME: GIANLUIGI ADAMOLI LOCATION: VERONA (ITALY)

INSTRUMENT: 235 mm SCT SEEING: Antoniadi scale I II [✓ III] [✓ IV] V

MAGNIFICATION: 270X TRANSPARENCY: very good good [✓ fair] poor

Figure 8. Observational record of Mercury by Gianluigi Adamoli.

are seen without making numerical estimates of brightness values, and this is also a legitimate way to record the observation. Figure 9 shows one of David Gray's fine drawings of Mercury.

Elong: 20°(W) d: 6.2" Ph: .71 i: 64.6°

2012 December 8d.08h.10m. UT. CM: 127°
Seeing: III / II-III (Antoniadi).
Transparency: Very Good
415mm Dall-Kirkham x365 (Binoviewer).
Filter: W#22 (Orange).
With Apodizer.

Figure 9. Drawing of Mercury by David Gray

The Italian amateur Mario Frassati is a skilled and dedicated observer of Mercury, and he has compiled a map, shown below, from his visual observations with a 20 cm Schmidt-Cassegrain. This is a remarkable achievement with a relatively small aperture, and shows what is possible with visual work.

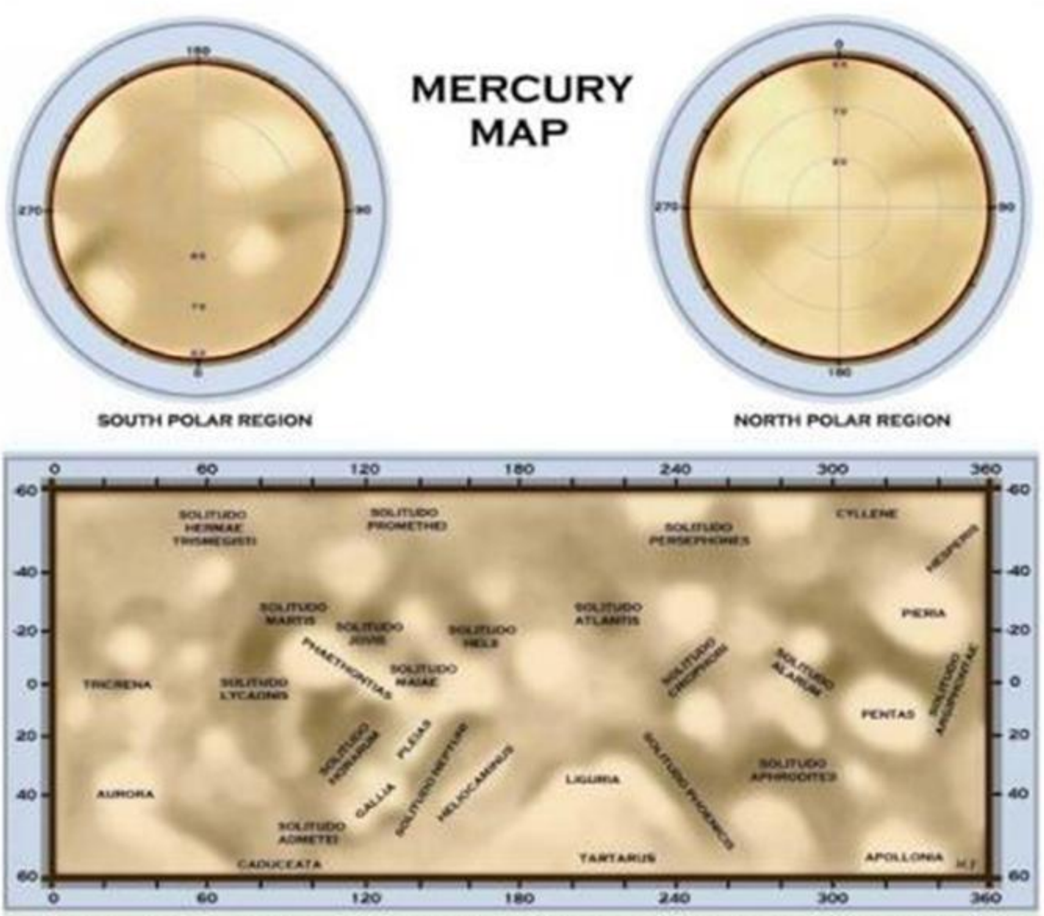

Figure 4. Chart of Mercury by Mario Frassati (Crescentino, Italy) from personal observations (203mm Schmidt–Cass). The chart covers the years 1997 to 2006.

Figure 10. Mario Frassati's map of Mercury, compiled from his visual observations and drawings.

6. Techniques for imaging Mercury

6.1 Introduction

It is probably fair to say that Mercury is one of the more challenging objects for planetary imagers, and this may explain why relatively few images are obtained. The small angular size, the low contrast of the surface features and the likely disturbance of the image by poor daytime seeing are the main obstacles to acquiring data of adequate quality to yield a good image. Even after the planet has been located visually, the process of getting an enlarged image onto the camera sensor ready to capture data is not trivial. The writer has developed a number of techniques for achieving this which may be helpful to imagers, and these are described later in the section.

6.2 Image scale and resolution

When Mercury is at a safe elongation of 10 degrees or more from the Sun, its angular diameter will be anywhere between 5 and around 10 arc seconds, with the larger diameters occurring during the crescent phases. 8 arc seconds is approximately the angular size of lunar craters of around 15 km diameter, whose shapes can be readily detected in images taken with amateur instruments. Images showing Mercury's phase can be obtained with relatively modest apertures, and the changing phases can be followed while Mercury remains far enough from the Sun.

In the remainder of this section, it will be assumed that the goal is to record surface features on Mercury, and this requires the best achievable resolution and a sufficiently large image scale. If a telescope of 250 mm aperture is used, the nominal angular resolution defined by the Rayleigh limit is around 0.4 arc seconds. This limit is based on the size of the Airy (diffraction) disc produced by the telescope optics, and strictly it applies only to the resolution of close double stars of equal magnitude, not to planetary detail. Experienced planetary observers and imagers are aware that details smaller than indicated by the Rayleigh limit can be detected, even if they are not fully resolved. Such features either have high contrast or are extended objects, and in either case there is a detectable variation in brightness or colour in the image. A good example is Cassini's division in Saturn's rings, which has an angular width of 0.75 arc seconds at the outer ends of the rings. It is a high-contrast feature, and can be seen visually in telescopes of only 80 mm aperture, for which the Rayleigh limit is around 1.2 arc seconds.

It is a general principle of imaging that to achieve the full resolution of the instrument, the image must be sampled at a minimum of 2 pixels per resolution element. For a 250 mm telescope, with a 0.4 arc second Airy disc, an image scale of 0.2 arc seconds per pixel would seem to fulfil the Rayleigh criterion. However, the pixel spacing along the 45 degree directions is 1.4 times greater than along the rows and columns, so to achieve 2 pixels per resolution element in those directions requires 3 pixels per resolution element in the horizontal and vertical, corresponding to a pixel size of 0.13 arc seconds. Several active imagers of Mercury, including the writer, use image scales in the range 0.1 to 0.15 arc seconds per pixel. Figure 11 shows how the pixel size in arc seconds varies with focal length for several different pixel dimensions, which do not necessarily correspond to those in actual planetary cameras, but represent the range of typical sizes. It is clear that a focal length of at least 4000 mm is needed to achieve the required level of sampling with small pixel sizes, and if the pixels are larger the focal length must be increased proportionally. If this seems too complicated, a simple rule-of-thumb developed by the experienced planetary imager Martin Lewis is to use an F/number close to five times the size of a pixel in microns. This applies to monochrome cameras in good seeing conditions. In poor seeing the F/number should be reduced to three times the pixel size in microns, allowing shorter exposure times. It is unlikely that the exact focal ratio given by this rule will be available for any given telescope and

Barlow lens combination, but observers can choose the combination that is closest for their equipment.

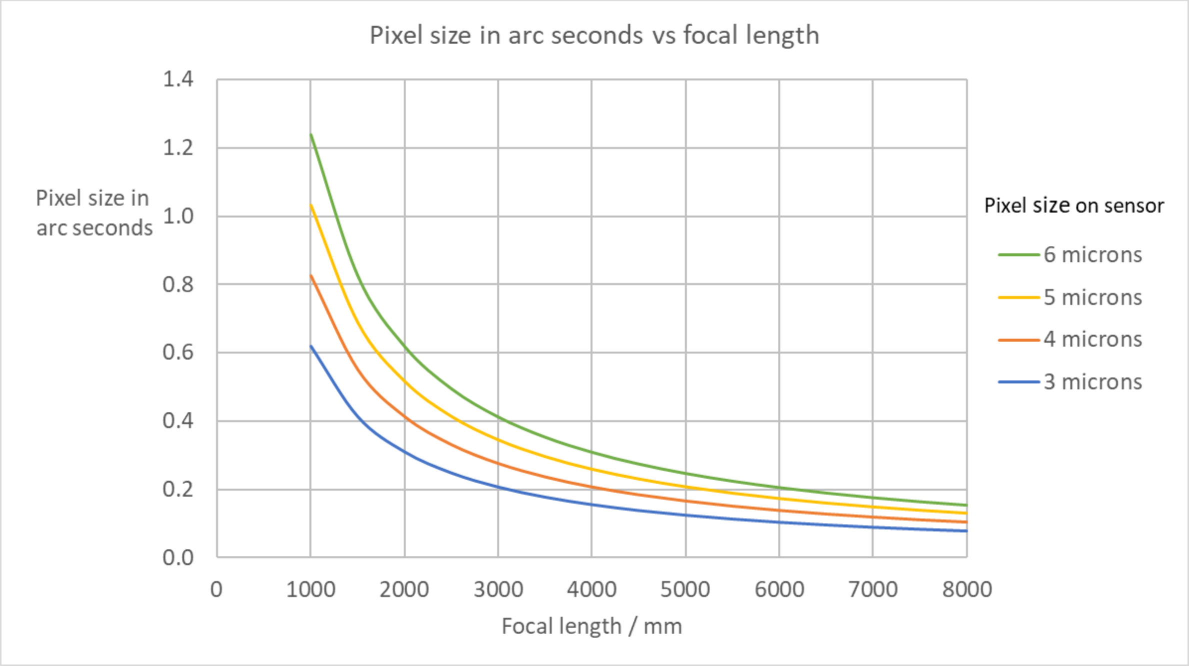

Figure 11. Pixel sizes in arc seconds for different focal lengths. The four lines correspond to different physical pixel dimensions on the camera sensor, which may not exist in actual cameras but can be used as a guide.

6.3 Barlow lenses and image magnification

Most amateur telescopes will require the addition of a Barlow lens or equivalent to increase the effective focal length of the instrument and obtain the required image scale. There are several types on the market at various price points. Normal Barlow lenses are usually just negative achromatic doublets, which are corrected for visible wavelengths because they are generally intended for visual observation. When used in the near infra-red, which is typically the case when imaging Mercury, they can introduce significant chromatic aberration. A Barlow lens designed and built by the writer for use in the near infra-red is described in Appendix 1. The Tele Vue Powermate^{TM} devices have a more sophisticated optical design and are better-corrected, and more expensive, than simple Barlow lenses.

The writer recommends making every part of the optical train parfocal. In other words, use parfocalising rings to set the camera and the eyepiece you use for finding Mercury to be parfocal with one another, and to ensure that when a Barlow lens is inserted before the eyepiece, the expanded image is in focus too. When imaging a bright planet at night, you can usually see the out-of-focus image after you add a Barlow, and it is easy to refocus and re-centre the image. When imaging Mercury in daytime, that is not the case. If you cannot, or choose not to, parfocalise everything, then it is a good idea to spend some time on a clear night observing the Moon or a bright star and measuring the changes of focus that are needed when switching from eyepiece to camera, and when adding the Barlow lens. If you know how far and in which direction to adjust the focus at each stage, it will make the process of setting up to image Mercury very much easier.

6.4 Filters

The majority of imagers use filters of some kind for Mercury. Although the albedo features can be seen visually, as described in Section 5, they tend to have greater contrast in the deep red and infra-red, and are recorded more clearly on images at those wavelengths. IR-transmitting filters are readily available, and some imagers use them for other planets, particularly the gas giants, where they can (for example) bring out features due to methane in the planet's atmosphere. Mercury has no significant atmosphere, and the purpose of the filter is mainly to increase the contrast of the bright albedo features around impact craters. A secondary benefit is that the image distortion due to atmospheric seeing is less at the red end of the spectrum, because any change of optical path due to turbulence is a smaller fraction of the wavelength in the red compared to the blue. Against this, however, both the resolution of the telescope and the sensitivity of the camera sensor decrease at longer wavelengths.

The writer started out imaging Mercury in the deep red and near-IR, using an IR-pass filter with a cut-on wavelength (50% transmission) of 685 nm. This filter transmits well beyond 1 micron wavelength, so the full sensitivity of the camera in the infra-red part of the spectrum is usable. Images acquired with a lighter red filter under excellent conditions showed less detail, even though the greater transmission of the filter and the increased sensitivity of the sensor to the shorter wavelengths allowed exposures that were three times less than with the IR-pass filter. After a lot of experimenting, the reason for this was found to be the chromatic aberration of the Barlow lens used to expand the image. Like most Barlows, it was designed for visual observation, and is a negative achromatic doublet corrected for the C and F lines to minimise the colour error in the visible. Its focal length in the near-IR varies significantly with wavelength, and this was the cause of the loss of quality in the images. The writer now prefers to use a red glass filter transmitting 610 nm and longer wavelengths, combined with a standard IR-cut filter that blocks wavelengths longer than 710 nm. Imaging in the band from 610 to 710 nm combines acceptable sensitivity of the camera with a reduced level of chromatic aberration, and the results using the combined filter are generally better than those with the IR-pass filter alone. The choice of filters is, of course, a matter of the observer's personal preference and experience, and good results can be obtained in a variety of ways.

6.5 Cameras

Any planetary imager interested in imaging Mercury will almost certainly have a suitable camera and the necessary software. The type of camera is not too important, e.g. whether it has a CCD or CMOS sensor, and what size the sensor happens to be. The most important factor is the pixel dimension, as discussed in section 6.2, because the image scale and the optimum focal length depend on it. The sensitivity of the camera to red and infra-red wavelengths is also important, given that most images of Mercury will be captured using a red or infrared filter. This information will either be supplied by the camera manufacturer, or can be found by searching online for the specifications of the sensor used in the camera. Another factor to consider, particularly if buying a new camera, is whether the shutter is "global" or "rolling". With the latter type the image is read out from the sensor line by line rather than as complete frames, and if the subject is moving in the frame, as is often the case with Mercury, the motion can introduce extra distortion.

Perhaps surprisingly, monochrome cameras are not always preferable to one-shot colour types. In some cases the filters in the RGB matrix in front of the sensor, which are there to separate the colour channels in the image, have very good transmission in the infra-red beyond about 800 nm. Simon Kidd, a regular imager of Mercury from the UK, uses a 742 nm cut-on filter with a colour camera and obtains excellent results. There is not much point in using one-shot colour cameras to obtain colour images, as the colour on Mercury is extremely subtle. Colour-enhanced images of the Moon do reveal compositional variations in the maria, and images from Messenger have done the same for Mercury. However, any imager who has the equipment and skills to produce similar results from Earth-based imaging of Mercury is in no need of the advice in this guide!

6.6 Practicalities of imaging Mercury

Once Mercury has been located visually, the next step is to add any image amplification device and obtain an image from the camera on the monitor screen. Removing the eyepiece, inserting a Barlow lens and then either the camera or the eyepiece again can disturb the telescope, and also change the weight distribution. The field of view at the required image scale may be only a few minutes of arc, so if the pointing of the instrument changes slightly, either because of the weight change or if there is any slight looseness between the elements of the imaging train, Mercury may no longer be in the field of view. Some tests on the Moon using the same components will soon show if there is any movement, how large it is and in which direction. The writer recommends acquiring Mercury visually in the eyepiece with the Barlow lens before switching to the camera, and learning where the image needs to be placed in order for it to appear subsequently in the camera field. As discussed in Section 4 on locating Mercury, it is useful to have a crosswire in the eyepiece to help the eye to focus, and this also provides a positional reference.

When imaging at night it is easy to see the computer screen, either in night-vision mode or at minimum brightness. Imaging Mercury in daytime is completely different, because even in shade the ambient daylight overcomes the brightness of the screen, making seeing and focusing the image very difficult. Some form of light shielding is essential to block the light and minimise reflections from surrounding objects (including the observer), so you can view the screen easily and adjust the settings of the camera and capture software. A stout cardboard box works well, provided it is laid on its side and is big enough to hold the monitor or laptop. Refinements include painting the interior of the box black and hanging a dark cloth screen over the open side to block external light. Given that the telescope pointing will be controlled while watching the image on the screen, it is essential to have the telescope drive controls within reach, and the capability for remote focusing, while not absolutely essential, will make imaging far easier. The writer's setup is shown in Figure 12, below: the home-made laptop box is made from MDF and has doors on both sides, hinged at the back, with a 1 cm gap at the bottom to allow cables to be led in and out.

Figure 12. The writer's computer box set up for imaging Mercury, with the dark cloth folded back. The telescope drive controller is inside the box beside the laptop, and the focuser control is next to the box on the right.

A few other recommendations, based on the writer's experience, are as follows. When replacing the eyepiece with the camera, support the camera cable on the telescope tube in some way, such as looping it over the finder bracket or the tube clamps, rather than allowing it to hang freely. If there is any breeze at all, a hanging cable may start to swing and cause significant image movement; it is also very easy to touch or pull the cable by accident and lose the planet altogether. Start with the camera field of view set to the maximum possible, rather than a small region of interest (RoI), as this makes finding Mercury easier. Once everything is set up to capture images, the RoI can be reduced to the smallest size suitable for the conditions. This will keep the file sizes small and increase the frame rate, but the optimum size of the RoI will depend on how much the telescope may be moving in the breeze. If the telescope shakes in the wind so much that the image disappears out of the frame at times, software such as Chris Garry's Planetary Image Pre-Processor (PIPP) can be used to reject the blank frames, but more of the images are likely to be blurred. If the image drifts out of the field, the first thing to do is to reset the camera's field of view to maximum, rather than start driving the telescope around. If the drift was slow, Mercury will probably still be in the larger field, and you can re-centre it easily. Orient the camera so that the RA direction is more-or-less parallel to the long side of the frame. This makes centring the image and correcting for drive rate errors much more intuitive. Once the Barlow and camera are in place, tighten the locking screws to prevent them moving, or the camera rotating, during the session. Imaging Mercury successfully requires capturing a lot of data, so the session is likely to be quite long. Be sure to check from time to time that the telescope tube is not about to come into contact with the tripod legs or other parts of the mounting.

6.7 Image capture

Mercury rotates so slowly that there is no time limit for capturing data in one session, unlike Mars, Jupiter or Saturn. It is even possible to combine data from two successive days, as the rotation of the planet in 24 hours is around six degrees in longitude, an amount which in average conditions is smaller than the resolution limit. The real limits are likely to be the weather and the observer's free time or patience. When imaging other planets or the Moon in average seeing conditions, the fraction of video frames selected for stacking to create the final image will typically be between 20% and 50%. For Mercury, the relatively poor seeing during daytime results in a far smaller proportion of usable video frames, rarely exceeding 1%, and more often less than 0.5%. A good image usually requires the stacking of 500 to 1000 frames, so the number that must be captured will be at least 50,000 to 100,000 and often more than that. Some of the stacking programs will not accept files larger than a certain size, which is why the RoI should be reduced to the minimum suitable for the conditions, and the number of frames in each video chosen so as not to exceed the file size limit. Keeping the RoI small will also maximise the frame rate, which for Mercury is unlikely to be limited by the exposure time.

The trade-off between exposure time and camera gain is one where every imager has their own preferences. The optimum, if there is such a thing, minimises the disturbance of individual frames by the seeing while not introducing too much noise into the image by the use of high gain. Shorter exposures will tend to freeze the motion of the image, and may increase the number of frames that are acceptable in terms of distortion. However, short exposures require higher gain, which results in more shot noise such that more frames have to be stacked to overcome that noise. Interestingly, it has been shown that the amount of residual noise in the stacked image depends only on the total exposure time of the stacked frames. For example, stacking 1000 images of 10 milliseconds exposure will give as good a result, in terms of noise, as stacking 2000 images of 5 milliseconds exposure, and the shorter exposures are likely to suffer less from distortion due to the seeing. The conditions that prevail at the time the data is acquired will dictate where the balance should lie, but as with any planetary observation, the best images will always be obtained when the seeing is good.

6.8 Image processing

It is beyond the scope of this observing guide to discuss image processing techniques in detail. There are many descriptions online and elsewhere that provide a wealth of information, and several of these are listed in the reference section. The following is an outline which should provide the would-be imager with enough information to make a start. The basic techniques for obtaining an image of Mercury from captured video frames are the same as for the other planets. The processes of image quality evaluation, sorting, alignment, stacking and sharpening are applied to the raw data just as they are for the Moon, Mars, Jupiter and other subjects. The difference with Mercury, as mentioned above, is that the quality of the raw data is markedly lower. The main reason for this is the effect of seeing. Irrespective of whether Mercury is being imaged low down in the twilight, or at higher altitudes during the day, the proportion of video frames that are sufficiently free from distortion and other atmospheric effects is typically 1% or less, and the challenge is to extract those frames from the far larger number in the captured data.

The long-standing workhorse program for planetary imagers is Registax, developed by Cor Berrevoets and improved in collaboration with expert imagers until the latest version, Registax 6, was released in 2011. From that point development has apparently stopped, although the software is still available to download. Other useful programs are Autostakkert!, written and maintained by Emil Kraaikamp and now in version 4, and PIPP, or Planetary Image Pre-Processor, written by Chris Garry. PIPP does not stack images, but works as a quality-sorting program to pre-select video frames prior to using one of the other programs for further quality assessment, alignment and stacking. Simon Kidd also uses PIPP for deBayering and monochrome conversion of the files from his colour camera. Quality-sorting algorithms usually work by evaluating edge sharpness or the presence of fine detail, and they can struggle with Mercury data because so many of the images are distorted. Chris Garry and Martin Lewis are collaborating on developing new algorithms that work by evaluating the shape of the image.

A possible sequence of operations that could be used to process a set of video data of Mercury is given here. This is based on the writer's experience but is by no means the only method; other imagers will have their own preferences.

1. Eliminate frames where Mercury was not in the frame, due to disturbance of the telescope by wind, or by passing clouds. This can be done in any video-editing program, such as VirtualDub. PIPP can also be set to reject frames that do not contain a planetary image.

2. Use PIPP to do a preliminary quality sort of the frames in each captured video, and crop each one to a standard size with the planet centred. Save a proportion of the sorted frames, in the region of 30% depending on the quality.

3. Process the saved videos in Registax 5, using Gaussian pre-blur of 1 (or at most 2) and the Gradient2 quality estimator. Select and save a subset of the sorted frames, based on their visual appearance. NOTE: Registax 6, which is the latest version, does not allow the user to choose the quality-estimation algorithm. Registax 5 is still available to download: see the link in section 9.

4. Concatenate the saved video segments into one, and process this again in Registax using the same settings. Select a subset of the frames and stack them.

NOTE: Some imagers prefer to perform steps 3 & 4 using Autostakkert!

5. Sharpen the image using the wavelets in Registax, or in some other image processing program, and save the result.

This procedure will give a good image if the original data was of good enough quality, which in practice means around 1% to 2% of the frames show a reasonably sharp disc of Mercury with a recognisable phase. If the proportion of good frames is only around 0.5% or even less, the quality of the best frames will generally not be so good. To obtain a reasonable image from such data, the best frames must be selected visually, since algorithms are apparently not yet as discerning as the human eye and brain.

The process of manual frame selection is time-consuming, but it is possible to extract an image of surprisingly good quality from very unpromising data. The basic procedure is to open the selected video files in an editing program such as VirtualDub, and step through the file frame by frame, marking runs of poor frames for deletion until a good frame is seen. The decision about whether or not to include a frame is based entirely on the overall shape of the image, as it is rare that any detail can be seen in individual frames. The selected good frames gradually accumulate at the start and the bad ones are deleted, until the end of the file is reached and the good frames are saved as a new short video clip. The selected clips are combined, and processed again in Registax to yield the final image.

7. Advanced imaging techniques and other observations

7.1 Introduction and a warning

The safety considerations discussed in Section 2, and the material presented in Sections 5 and 6, have assumed that Mercury can be observed only under certain restricted conditions. In particular, it was emphasised that for any given telescope and light-baffle combination there is a minimum elongation at which the planet can be observed safely. This section deals with extending the period over which Mercury can be observed by relaxing those safety restrictions in a controlled way. This allows Mercury to be observed or imaged when it is closer to the Sun, but the consequence is a potentially greater risk to observers or their equipment. The writer strongly recommends that the methods described are used ONLY by experienced observers. It is essential to consider the risks very carefully before deciding to make observations of this sort.

WARNING: Do not attempt the observations described below unless you have the appropriate telescope, are aware of all the risks, are completely comfortable with the techniques for mitigating them and are confident that you can make the observations safely.

7.2 Levels of safety in observing Mercury

The highest level of safety is to observe Mercury only when the Sun is below the horizon. The second level, described in earlier sections, is to ensure that no sunlight is collected by the telescope optics. In the third level, we allow some sunlight to be collected, but ensure that no image of the Sun is formed. In practice this means that all of the cone of sunlight proceeding towards the focus is intercepted by the inside of the telescope tube. The result for a refractor will be heating of the inside of the tube and the internal baffles, rather than just the external light baffle. In a Newtonian, sunlight will fall on part of the primary mirror and be reflected onto the inside of the tube. The partial illumination of the mirror is likely to cause local changes of figure, and the warming of the inside of the tube will generate some convection currents. Both of these effects will degrade the image of Mercury. However, no image of the Sun will be formed with either instrument, so the risk of damage to the observer's eye or camera is still small.

The fourth and final level is to allow an image of the Sun to be formed, but to ensure it is in a place where it does no harm. This is not possible with a refractor, and is extremely difficult with compound telescopes having short-focus primary mirrors. With a Newtonian, the image is formed in mid-air above the entrance to the tube, and provided the focusing cone of sunlight does not hit the top of the tube, the spider or the edge of the secondary mirror, and the telescope is not disturbed, the situation is relatively safe. In fact, this configuration may give a better quality image than the third level, because the primary mirror is likely to be fully in sunlight, and the heating will be more or less uniform. The result will be mainly a change of focal length, which can be compensated for, rather than the distortion of the image that can occur if the mirror is sunlit only on one side. The reflected light does not strike the inside of the tube, so there will be less heating and convection to disturb the image.

The techniques presented in more detail in this section involve the use of the third and fourth levels of safety described above.

7.3 Imaging Mercury close to the Sun

Using a light-baffle with an L/D value in the region of 5, which is not too unwieldy and provides a fair level of screening, Mercury can be observed any time it is further than 11 degrees from the Sun. To observe the planet at smaller elongations, either a longer baffle must be used, or the requirement for collecting no sunlight must be dropped. Provided that the sunlight never reaches focus, there is still no image of the Sun. In the case of a Newtonian, the geometry ensures that the sunlight focused by the mirror intercepts the tube at a very oblique angle, spreading the energy over a large area. Refractors often have a series of light-baffles inside the tube, and the light will hit one or more of these, thereby distributing the energy along the tube, although the intensity on a given baffle, especially those near the eyepiece, will be higher because the light hits it almost square-on. Figure 13 shows typical conditions for safety level 3 in a refractor and a Newtonian.

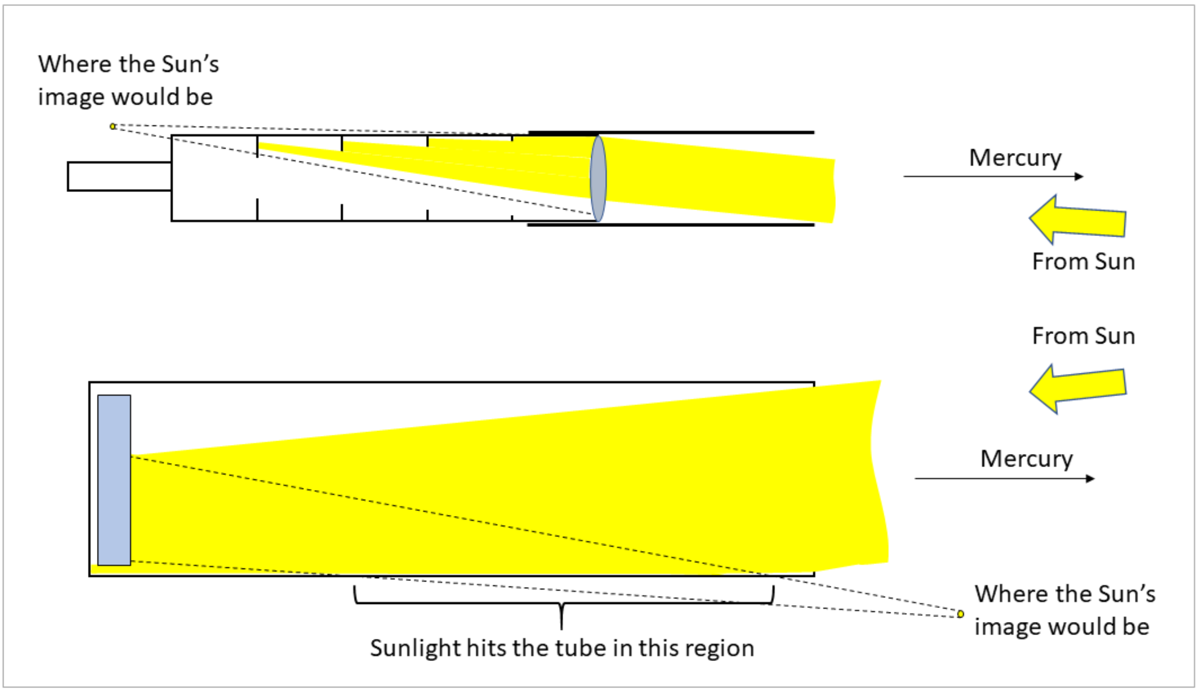

Figure 13. Optical diagrams of a refractor and a Newtonian illustrating the condition in which some sunlight enters the telescope when Mercury is being observed. The places where the Sun's image would be formed are shown, although no light reaches them.

The only significant difference between imaging in these circumstances and those described in Section 6 is that there will be more heating of the inside of the telescope tube and, for the Newtonian, the primary mirror will be partly in sunlight. Mirror coatings are never perfectly reflective, so some of the sunlight will be absorbed, and the uneven heating and expansion of the mirror is likely to degrade the image: there is nothing that can be done about this. Running the mirror cooling fan will not help, because the heat is absorbed at the front of the mirror, and the thermal conductivity of glass is low.

The heating of the tube may be more significant for a refractor where the tube is sealed and the heat cannot escape, because most refractors are not fitted with cooling fans. The writer has experimented with cooling the outside of a (metal) Newtonian tube by wrapping it in a piece of old sheet and spraying it periodically with water. No improvement of the image was noticed, but the tests were not performed in a very systematic way, and further trials would be worthwhile. This approach could also be tried with a refractor.

The closer Mercury approaches to the Sun, the closer the cone of sunlight comes to the end of the telescope tube. For a refractor this represents the limit of observation, because allowing sunlight to enter the drawtube would be very unwise. The heat and light are becoming highly concentrated, and there is a real risk of damaging the instrument by scorching the interior black paint or melting plastic components of the tube. The minimum elongation angle at which Mercury can be observed depends on the focal length and other characteristics of the particular telescope, and must be worked out in each case. Observations of Mercury at very small elongations are only feasible with a Newtonian.

7.4 Imaging Mercury near superior conjunction

Before explaining how Mercury can be imaged close to superior conjunction, it is worth considering why we might wish to do so. Aside from the challenge, there is one important reason, which is that the planet is at 100% phase, or very close to it, and the brightness gradient across the visible disc is minimised. One of the difficulties with imaging Mercury is the wide range of illumination, ranging from maximum near the limb to zero at the terminator. Imaging the whole of a quarter or gibbous Moon presents the same problem: the dynamic range of the camera may not be wide enough to capture the full range of brightness, so that parts of the image are either saturated or underexposed. Most lunar images aim to record fine detail in small regions where the range of illumination is not too great. In contrast, we always image the whole visible face of Mercury, so the full range of brightness is present. Near superior conjunction there is a chance to capture an entire hemisphere of the planet under conditions where the apparent brightness is uniform apart from the albedo features on the surface.

For any given Newtonian telescope there will be a limited range of elongations at which Mercury can be imaged under the conditions that satisfy the fourth level of safety defined above. These are illustrated in Figures 14 and 15. As in the previous figures, the telescope is assumed to be aimed at Mercury, and we are considering where the sunlight reflected from the primary mirror goes. In this case there is an image of the Sun, formed somewhere beyond the open end of the telescope tube.

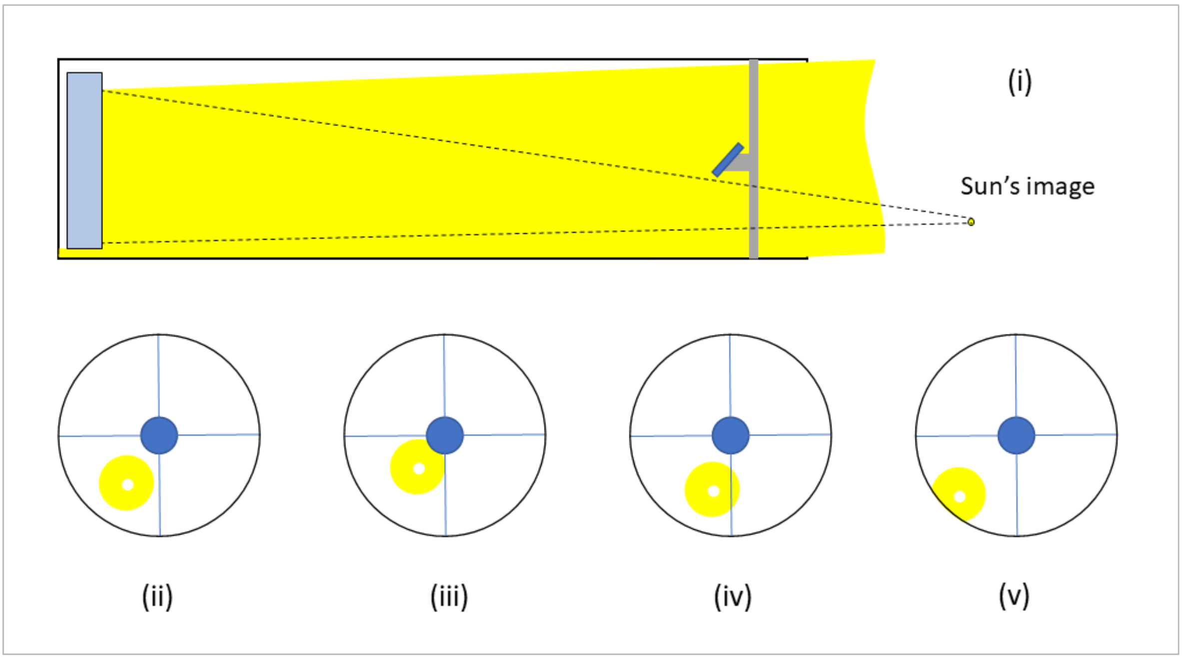

Figure 14. Using a Newtonian to image Mercury near superior conjunction. (i): side view of the telescope and light-cone; (ii) to (v): views of the front of the tube. (ii) Safe position of the light-cone in the aperture; (iii) unsafe position of the light-cone; (iv) and (v) positions of the light cone that are not recommended.

The first consideration, and the one that is essential for safety, is that no part of the light-cone hits the secondary mirror. The writer regards this as an unbreakable rule: any light reflected by the secondary will produce an image of the Sun in the field of view and present a serious hazard. This situation is shown in Figure 14 (iii) above. Parts (iv) and (v) of the figure, where sunlight hits either the secondary support or the inside of the top of the tube, are also undesirable because of the heating that will result, although a small cut-off of the edge of the cone as in (v) may be acceptable. Parts (i) & (ii) of the figure show the cone of sunlight emerging fully from the top of the tube, and this is the condition under which Mercury can be imaged safely. The range of elongations over which this condition applies must be calculated for each individual instrument based on the focal length and the tube dimensions. For the writer's telescope, a 250 mm F/6.3 Newtonian, the minimum elongation angle is 2.25 degrees and the maximum is about 4.25 degrees. The details of the calculation are included in Appendix 2 for those who wish to work out the angles for their own telescope. These angles define an annular region centred on the Sun where Mercury can be imaged for a few days as it moves through conjunction, as shown in Figure 15, which is drawn to scale for the telescope described. The red circle is the no-go region where the sunlight cone would be intercepted by the secondary mirror, and the light green area is where Mercury can be imaged using the precautions described. The green lines are some possible paths of Mercury as it passes through conjunction. Depending on the minimum elongation distance, there can be either a single period of up to six days, or two periods of from two to five days each, during which Mercury is within the green region. The lengths of those periods also depend on whether the planet is near perihelion or aphelion at the time of conjunction.

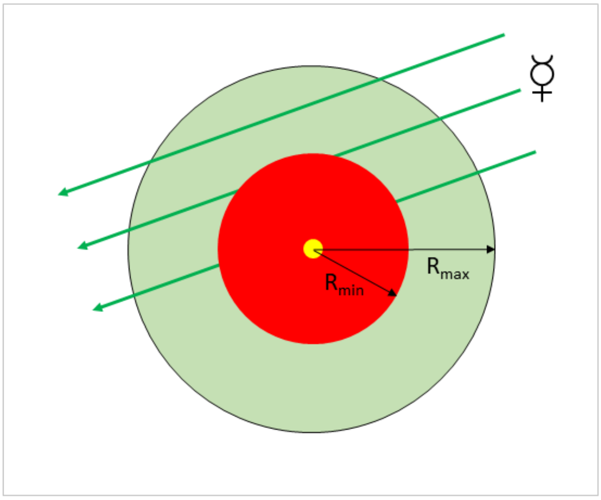

Figure 15. The region near the Sun showing the annular zone (in green) where Mercury can be imaged near conjunction, with appropriate precautions.

Mercury can be located when near the Sun in the same way as described in Section 4, with some additional precautions due to the Sun's proximity. The writer strongly recommends preparing and using a checklist of the steps to be followed. Breeze or wind, especially if strong or gusty, should be a concern: if it is strong enough to move the telescope appreciably and cause the image to move off the sensor, it would be wise to consider waiting, or abandoning the session altogether, to avoid the risk of damaging the camera. Finding Mercury will be possible only if the sky is very transparent, and there is no high cloud or haze. Mercury may be as bright as magnitude -2, but any slight enhancement of the scattering of sunlight near the Sun by atmospheric effects will prevent it from being seen.

The procedure in Section 4.2 is used up to step 7. After slewing to Mercury's predicted position and removing the solar filter, the new step 8 is to hold a strip of white card near the front of the tube, locate the sunlight cone and confirm there is no sharp edge due to it hitting the secondary. If one can be seen, Mercury is too close to the Sun for safe imaging, and the attempt must be abandoned. If the sunlight cone is hitting one of the secondary supports, replace the solar filter, rotate the tube far enough for the cone to be unobstructed, and repeat the first steps of the process. Having confirmed the sunlight cone is exiting the tube cleanly, the observer can attempt to find Mercury in the eyepiece. Some may prefer to omit the step of visual acquisition, and use the camera to locate and centre the image before adding the Barlow lens. Once the planet has been located and the image is on the monitor, the process of image capture is the same as at any other time. The background sky will be much brighter due to the increased amount of scattered sunlight, and the optimum gamma and exposure settings may be significantly different from those used when imaging at greater elongations.

Opportunities to image Mercury near conjunction are rare because multiple conditions must be satisfied at the same time. The writer has imaged the planet successfully in this way on only three occasions over the last four years. Given the difficulties, however, capturing an acceptable image at conjunction is a very satisfying achievement.

7.5 Imaging Mercury's sodium tail

Mercury's proximity to the Sun means that its surface temperature can reach over 400 degrees Celsius on the dayside. The surface is also bombarded by micrometeorites, the solar wind and occasionally by coronal mass ejections. The bombardment produces a very tenuous exosphere consisting of the lighter elements from Mercury's crust, including helium, oxygen, sodium, potassium and calcium, which are vaporised or sputtered from the surface rocks. Sodium is one of the main constituents of this exosphere. After leaving the surface, the sodium and other atoms can be accelerated by solar radiation pressure into a narrow tail resembling that of a comet. In fact, some comets are observed to have sodium tails, or at least to have detectable quantities of sodium in their ion tails. Sodium atoms have a significantly larger cross-section for absorption and re-emission of sunlight than the other atomic species that are present, thus the tail is brightest at the yellow sodium wavelengths.

The formation and excitation of the tail both depend on the absorption of sunlight by the sodium atoms in the exosphere. However, sunlight itself has absorption lines due to sodium (the D lines) at wavelengths of 589.0 and 589.6 nm. Figure 16 (a) shows a schematic of the solar spectrum near one of these absorption lines, with the red dashed lines indicating the absorption window of the sodium atoms. When Mercury's radial velocity is close to zero near perihelion or aphelion, the absorption window overlaps the solar absorption line, so relatively little light is available to be absorbed by the sodium atoms.

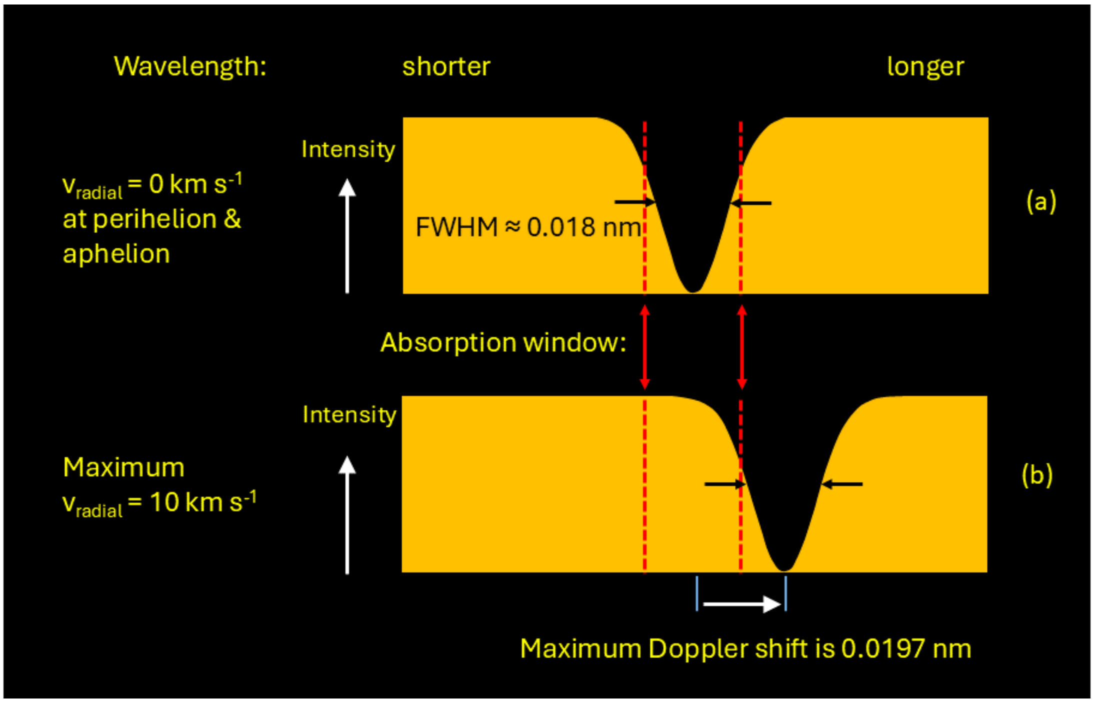

Figure 16. Doppler shift and absorption of sunlight by sodium atoms in Mercury's exosphere and tail. (a) With zero Doppler shift at perihelion or aphelion. (b) Maximum red shift sixteen days after perihelion.

As Mercury moves away from perihelion, its radial velocity increases due to the eccentricity of its orbit, and this results in a Doppler shift of the solar spectrum. The maximum radial velocity of 10.06 km s^{-1} is reached 16 days after perihelion. The Doppler shift is then 0.0197 nm, which is slightly more than the width of the solar absorption lines, as shown in Figure 16 (b). At that point there is ten times more sunlight in the absorption window than at perihelion or aphelion, and the tail is strongly excited. The tail first becomes detectable between 4 and 5 days after perihelion, when enough sunlight can be absorbed for the sodium atoms to be readily ejected from the exosphere. Photons that are absorbed transfer their momentum to the sodium atoms and accelerate them directly away from the Sun. This increases their radial velocity, which in turn increases the Doppler shift. When the excited atoms return to the ground state they re-emit the light at the same wavelengths but in random directions, which on average does not change the velocity of the atoms. The re-emitted light can be detected by imaging through a filter that transmits the sodium wavelengths.

Although Mercury's maximum radial velocity is 10.06 km s^{-1} either after or before perihelion, the situation before perihelion is less favourable for the development of a tail, because at that point in its orbit Mercury is moving closer to the Sun. The sunlight is thus blue-shifted, not red-shifted as it is after perihelion. Radiation pressure again accelerates the sodium atoms away from the Sun, but that now reduces their radial velocity. The result is greater overlap between the solar D lines and the absorption window of the sodium atoms, so their acceleration is reduced. Consequently, the tail is shorter and fainter before perihelion than after perihelion. This asymmetry favours observation of the tail from the northern hemisphere, because Mercury moves north of the ecliptic shortly before perihelion passage and is better placed for northern hemisphere observers when the tail has its greatest extent.

Mercury's tail was detected in ground-based images by Baumgardner *et al* [1] in 2008. They used a 10 cm refractor configured as a coronagraph, i.e. with an occulting disc in the focal plane to block the bright image of Mercury, and a narrow-band filter transmitting the sodium wavelengths. The observations were made in twilight with Mercury about 5 degrees above the horizon, to minimise the background light scattered by Earth's atmosphere and the emission from the atmospheric sodium layer at 90 km altitude. The recorded extent of the tail was 1.5 degrees, which corresponds to about 1400 radii of Mercury or 3.4 million km. The velocity of the sodium atoms is so high that they travel that distance away from the planet in less than a day. Baumgardner *et al* note that if variations in brightness along the tail could be detected, they would provide a record of changes in the loss rate from the exosphere due to variations in the solar wind, coronal mass ejections or meteoroid impacts.

The periods when Mercury's tail can be observed are infrequent and generally short because several factors must combine favourably. First, Mercury must be within about 10 days of greatest elongation. Second, it must be visible at an altitude of 3 degrees or more (to minimise extinction) in a dark or twilight sky with the Sun at least 10 degrees below the horizon. This restricts the observations to times when the ecliptic is at a sufficiently steep angle to the horizon, which are generally spring evenings and autumn mornings. Third, as described above, Mercury must be in a part of its relatively eccentric orbit where it is approaching or (preferably) receding from the Sun. Finally, and by no means least, the sky must be clear and transparent down to the horizon in the relevant direction.

The observations do not require a large aperture, but a fast optical system (i.e. a small F/number) is essential to give an image of the tail that is bright enough to record and to ensure an adequate field of view. A small refractor working at F/6 or less would be a good starting point if combined with a camera giving a field of one degree. The sodium tail has been imaged without using either a narrow-band sodium filter or an occulting bar, but only in extremely transparent skies from locations in southern Europe. For imaging from the UK the writer has always used a sodium bandpass filter to eliminate as much of the sky background as possible and improve the contrast of the tail. Filters with 10 nanometre bandwidth are fairly standard, and available from suppliers such as Thorlabs and Edmund Optics. One of these would be good enough for the purpose. There are a few sources of narrower-band filters, but the cost tends to escalate rapidly as the bandwidth decreases. The writer first imaged the tail using a filter with 3.5 nm bandwidth, obtained from Knight Optical in the UK.

The use of an occulting block has both advantages and disadvantages. The advantage lies in reducing the glare from Mercury, which will inevitably be severely overexposed due to the long exposures (tens of seconds) required for the tail. The disadvantage is the added complexity of the imaging setup needed to use such a block. The best block is a strip of attenuating filter such as aluminised Mylar which will reduce the brightness of Mercury in the image without blocking it completely. This eliminates the glare and allows the position of Mercury to be found accurately, which is important for measuring, say, the width of the tail at different distances from the planet. There are two options for adding such an occulting strip.

Most planetary cameras have a protective window which is several millimetres from the sensor, and if the attenuating strip is placed there it will be a long way out of focus and appear very blurred in the image. However, if the user is prepared to open the camera housing and fix the strip on the cover of the sensor itself, it will only be slightly out of focus and the results will be usable. Great care should be taken when doing this as there is a risk of damaging the camera, and any warranty may be voided.

The second option requires additional optics. The filter strip should be positioned at the focus of the telescope, and at least one extra lens will be needed to relay the focal plane onto the sensor so that everything is sharp. The observer must buy or make an optical system that can do this. The simplest option would be a commercial macro lens of sufficient aperture to accept the focal cone from the telescope: such lenses are designed and corrected for close-up imaging, which is the exact situation we are considering, and using one would also decrease the F/number. Someone with experience of constructing optical equipment could make a customised device such as the one shown in Figures 17 and 18 below, which was built by the writer for this purpose.

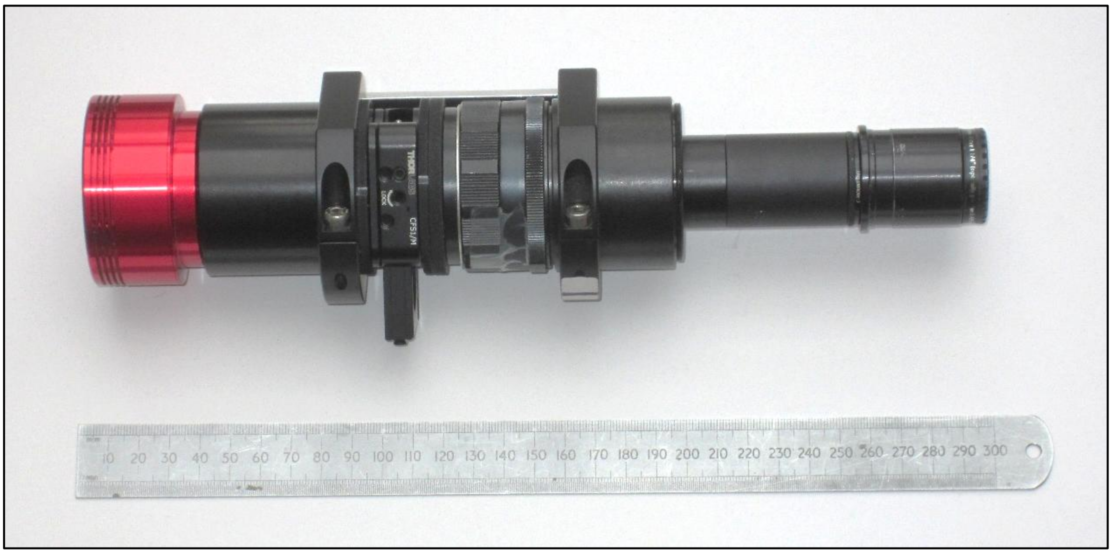

Figure 17. Re-imaging system used for Mercury's sodium tail. The device weighs 850 grams.

The optical system shown above uses an old 55 mm F/2 camera lens and a modern 25 mm F/1.4 CCTV lens, mounted facing one another. The mounting hardware consists of 1-inch and 2-inch diameter lens tubes and thread adapters bought from Thorlabs. The two lenses relay the image plane of the telescope where the filter strip is positioned onto the camera sensor with a 0.45x magnification, thus increasing both the image brightness and the field of view. The sodium filter is mounted in a slide between the lenses. A bracing bar between the two parts of the device eliminates a slight movement due to the focusing action of the 55 mm lens. This device was originally made for a different project which required imaging at two wavelengths, and the slide holds both filters to allow a quick change between them. If instead a single macro lens is used for re-imaging as suggested above, placing the filter in the focal cone of the telescope a few centimetres from the focus will not cause any problems except with the narrowest bandpass filters, which are sensitive to the angle of incidence.

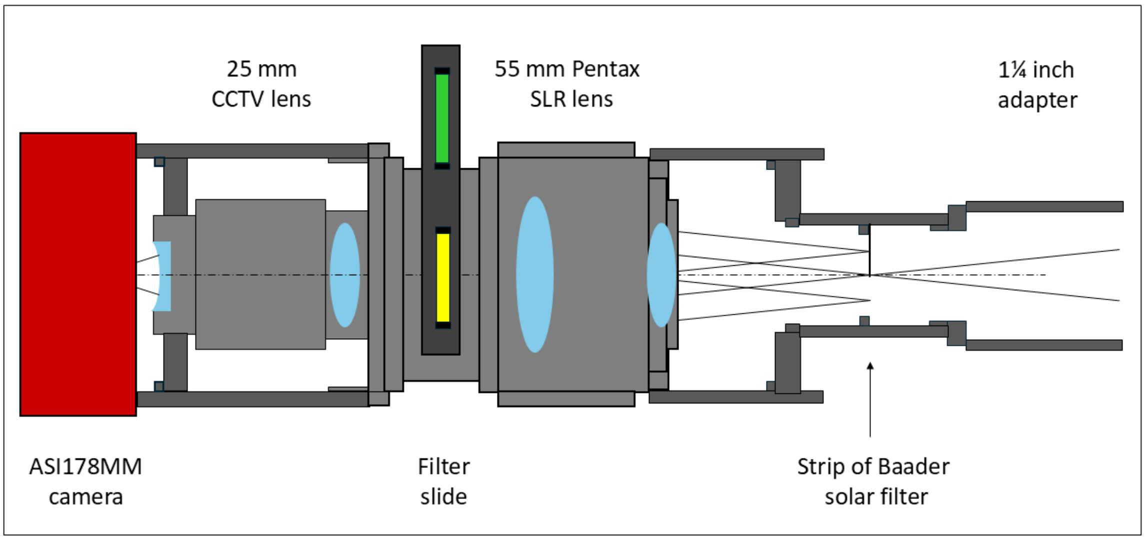

Figure 18. Schematic of the re-imaging system with the principal components labelled.

A planetarium program can be used to determine the best times to image the tail. *Stellarium* gives the distance of Mercury from the Sun: the minimum is 0.308 astronomical units at perihelion, and there are normally four consecutive dates showing it at that distance. The tail becomes detectable approximately five days after perihelion, so you can find the position of Mercury from your location to work out the best time period for observing. Mercury is brightest at superior conjunction, so is easiest to locate in the twilight in the two weeks after it reappears in the evening sky. Depending on the date of conjunction, however, the tail may be at its brightest after Mercury has become quite faint, and in those circumstances an occulting bar may be unnecessary. More details about the observational procedure and some of the writer's images of the tail can be found in issues Nos 10 and 15 of *Messenger*, the Mercury and Venus Section newsletter, which BAA members can download from the Section webpage.

There are some example images showing Mercury's tail in the Gallery section of this guide. In many respects recording the tail is similar to deep-sky imaging: the faintness of the tail means that exposures of several tens of seconds are needed and some form of autoguiding is almost essential. Given that many amateur astronomers are regular deep-sky imagers, it is clear that imaging Mercury's tail is a challenge that those who are interested should be well-placed to undertake. In addition, there is the potential for a collaboration with professional astronomers and space scientists. The Japanese and European Space Agencies' Bepi-Colombo probe to Mercury was launched in October 2018 and is now scheduled to arrive at Mercury in November 2026. That interval provides a window for studying the behaviour of the sodium tail and how it reacts to solar events, so that a base of knowledge is built up before the spacecraft arrives in orbit around Mercury.

Reference:

1. Jeffrey Baumgardner, Jody Wilson and Michael Mendillo, 'Imaging the sources and full extent of the sodium tail of the planet Mercury', GEOPHYSICAL RESEARCH LETTERS, VOL. 35, L03201, doi:10.1029/2007GL032337, 2008

Free download from: https://agupubs.onlinelibrary.wiley.com/doi/full/10.1029/2007GL032337

8. Gallery of observations

8.1 Introduction

This section of the guide presents a selection of observations and images of Mercury taken from the archives of the BAA Mercury and Venus Section. They are intended to showcase the work of past and present members of the Section, and give new observers an idea of the results that can be achieved at an amateur level. The archive contains a great deal of material, much of which is of high quality, so the writer was forced to be very selective to keep this section to a reasonable length. Only one example of work by each contributor is included here, so unfortunately many fine drawings and images had to be excluded. The drawings and images are presented unedited and uncropped in most cases, so that the notes and comments made by the observer are included.

8.2 Visual observations and drawings

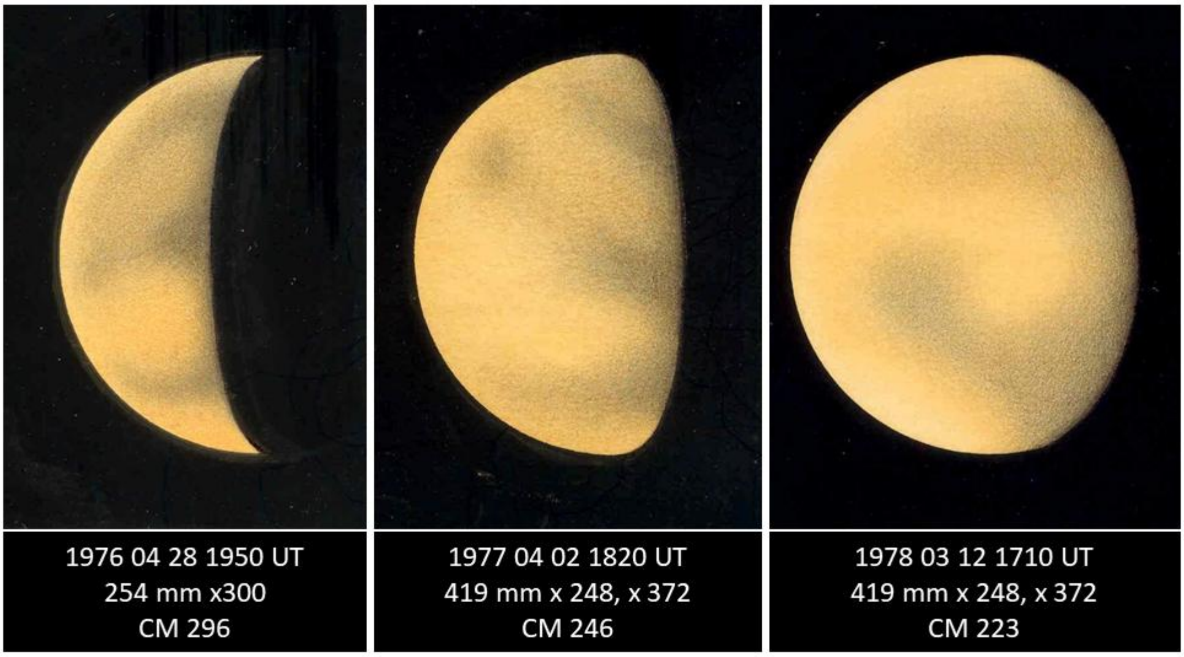

Figure G1. Montage of drawings by Paul B Doherty from 1976 to 1978. Doherty described the view on April 2nd 1977 as "my best ever view".

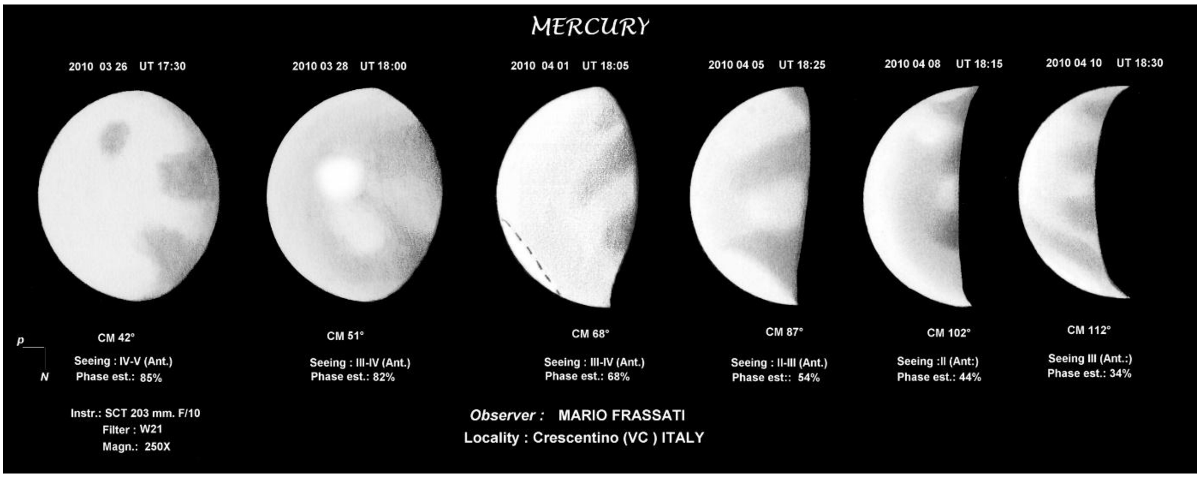

Figure G2. Montage of images by Mario Frassati from March and April 2010.

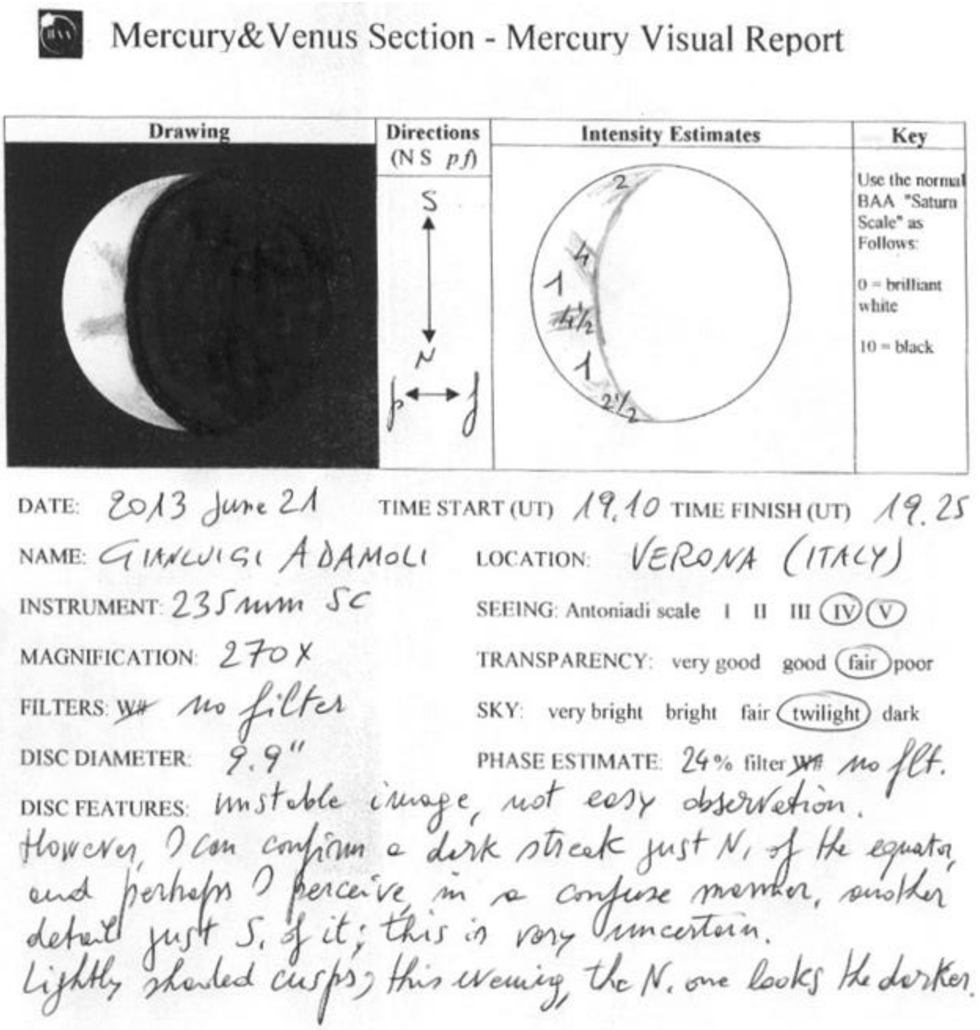

Mercury&Venus Section - Mercury Visual Report

Drawing	Directions (N S p f)	Intensity Estimates	Key
			Use the normal BAA "Saturn Scale" as Follows: 0 = brilliant white 10 = black

DATE: 2013 June 21 TIME START (UT) 19.10 TIME FINISH (UT) 19.25

NAME: GIANLUIGI ADAMOLI LOCATION: VERONA (ITALY)

INSTRUMENT: 235 mm SC SEEING: Antoniadi scale I II III [✓ IV] [✓ V]

MAGNIFICATION: 270 X TRANSPARENCY: very good good [✓ fair] poor

FILTERS: ~~W#~~ no filter SKY: very bright bright fair [✓ twilight] dark

DISC DIAMETER: 9.9" PHASE ESTIMATE: 24% filter ~~W#~~ no flt.

DISC FEATURES: unstable image, not easy observation. However, I can confirm a dark streak just N. of the equator, and perhaps I perceive in a confuse manner, another detail just S. of it; this is very uncertain. Lightly shaded cusps; this evening, the N. one looks the darker.

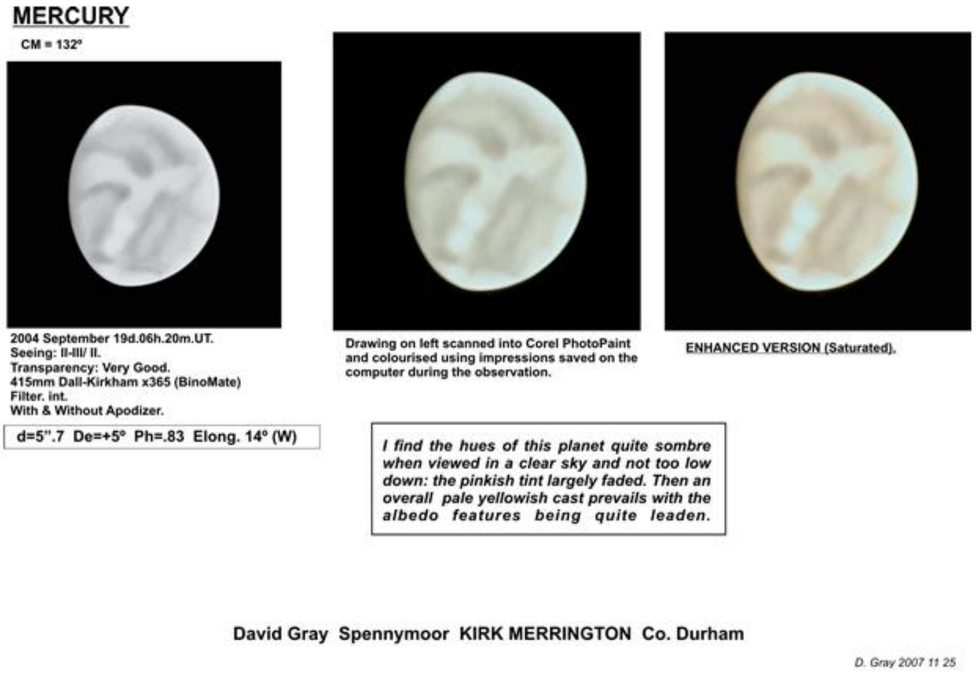

MERCURY

CM = 132°

2004 September 19d.06h.20m.UT.
Seeing: II-III/ II.
Transparency: Very Good.
415mm Dall-Kirkham x365 (BinoMate)
Filter. int.
With & Without Apodizer.

d=5".7 De=+5° Ph=.83 Elong. 14° (W)

Drawing on left scanned into Corel PhotoPaint and colourised using impressions saved on the computer during the observation.

ENHANCED VERSION (Saturated).

I find the hues of this planet quite sombre when viewed in a clear sky and not too low down: the pinkish tint largely faded. Then an overall pale yellowish cast prevails with the albedo features being quite leaden.

David Gray Spennymoor KIRK MERRINGTON Co. Durham

D. Gray 2007 11 25

Figure G3. An observing report by Gianluigi Adamoli and a set of drawings by David Gray.

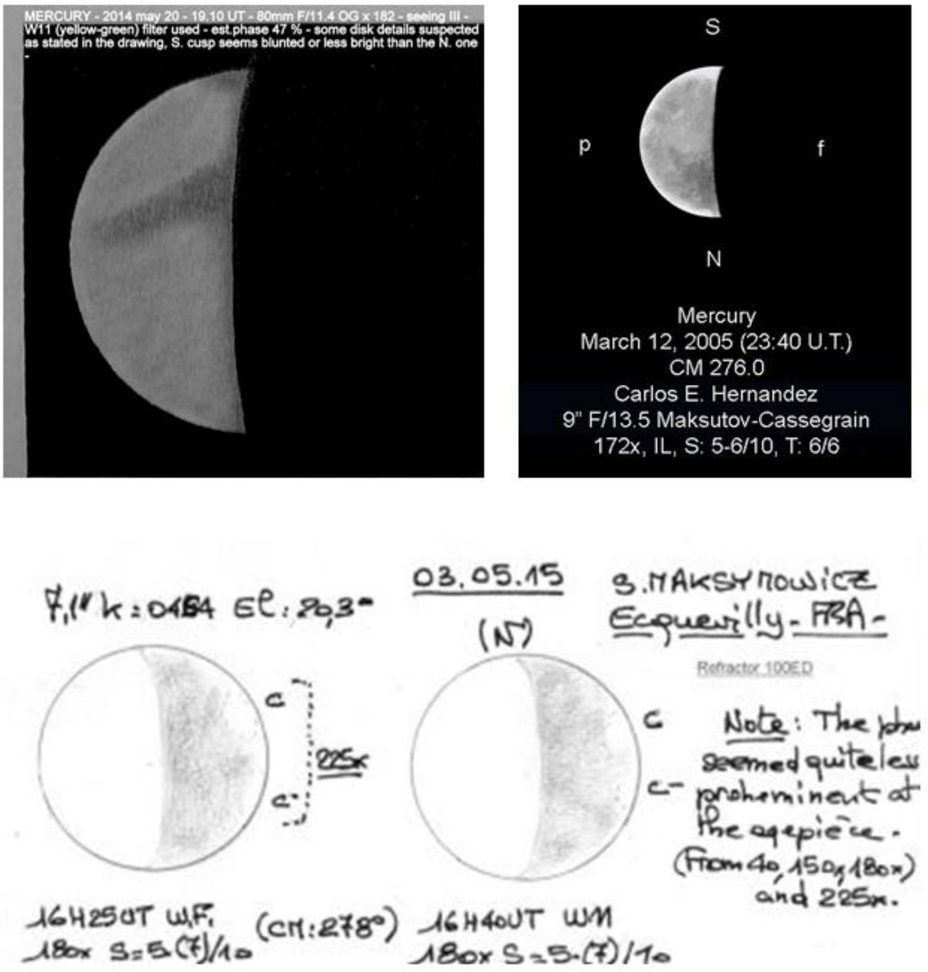

MERCURY - 2014 may 20 - 19.10 UT - 80mm F/11.4 OG x 182 - seeing III - W11 (yellow-green) filter used - est.phase 47 % - some disk details suspected as stated in the drawing, S. cusp seems blunted or less bright than the N. one -

Mercury
March 12, 2005 (23:40 U.T.)
CM 276.0
Carlos E. Hernandez
9" F/13.5 Maksutov-Cassegrain
172x, IL, S: 5-6/10, T: 6/6

03.05.15
S.MAKSYMOWICZ
Ecquevilly - FRA -
Refractor 100ED
7,1" k: 0.484 El: 20,3°
16H25UT W.F. 180x S=5(7)/10
(CM: 278°)
16H40UT WM 180x S=5-(7)/10

Note: The [illegible] seemed quite less prominent at the eyepiece. (From 40, 150x, 180x) and 225x.

Figure G4. Drawings of Mercury by Massimo Giuntoli, Carlos Hernandez and Stanislas Maksymovich.

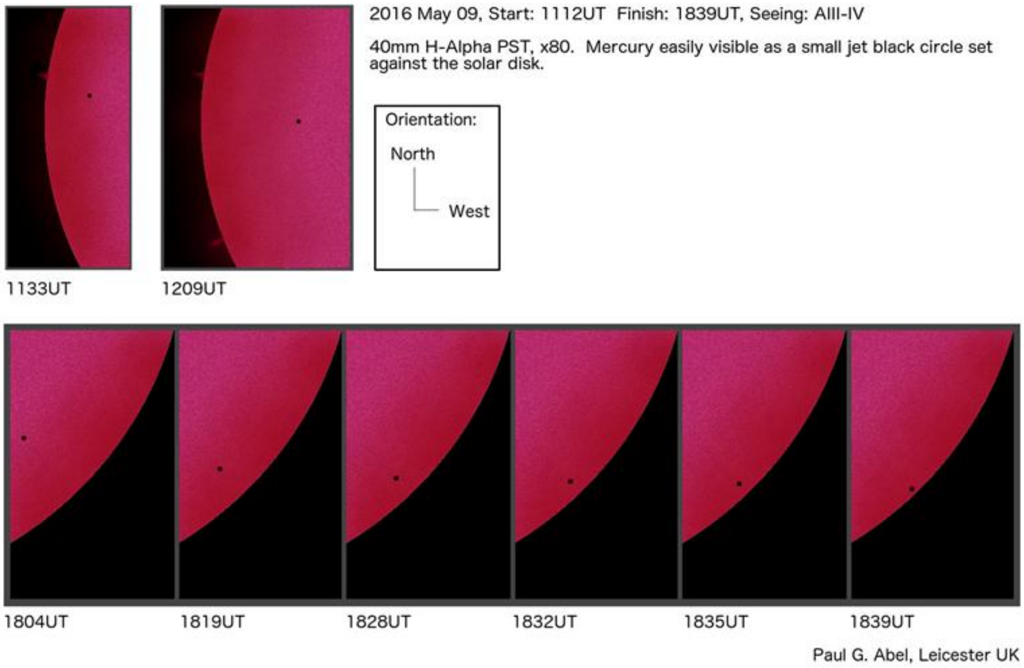

2016 May 09, Start: 1112UT Finish: 1839UT, Seeing: AIII-IV

40mm H-Alpha PST, x80. Mercury easily visible as a small jet black circle set against the solar disk.

Paul G. Abel, Leicester UK

Figure G5. Drawings by Paul Abel of the 2016 transit of Mercury in hydrogen-alpha light.

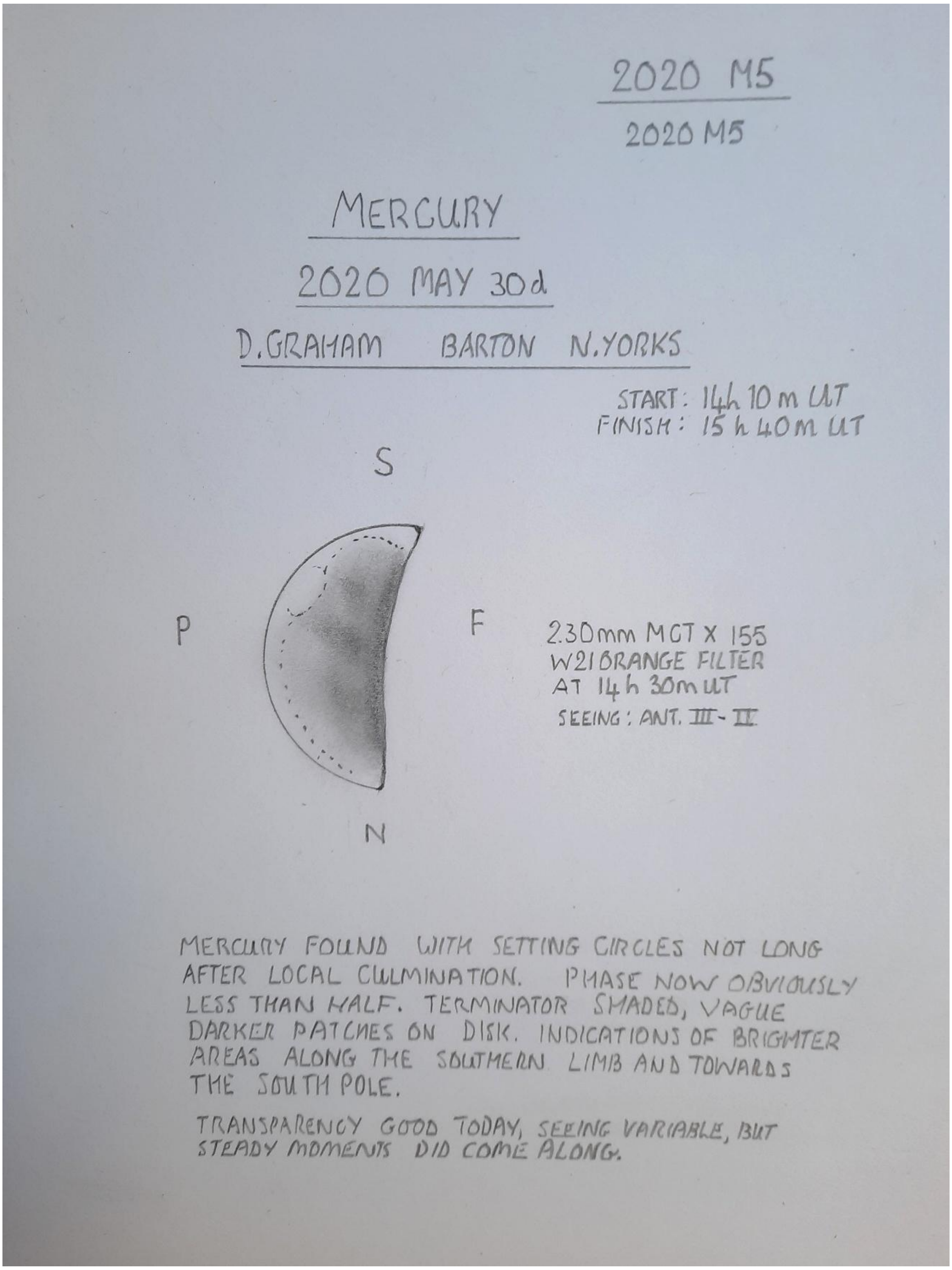

2020 M5

2020 M5

MERCURY

2020 MAY 30d

D.GRAHAM BARTON N.YORKS

START: 14h 10 m UT
FINISH: 15 h 40m UT

230mm MCT X 155
W21 ORANGE FILTER
AT 14h 30m UT
SEEING: ANT. III - II

MERCURY FOUND WITH SETTING CIRCLES NOT LONG AFTER LOCAL CULMINATION. PHASE NOW OBVIOUSLY LESS THAN HALF. TERMINATOR SHADED, VAGUE DARKER PATCHES ON DISK. INDICATIONS OF BRIGHTER AREAS ALONG THE SOUTHERN LIMB AND TOWARDS THE SOUTH POLE.

TRANSPARENCY GOOD TODAY, SEEING VARIABLE, BUT STEADY MOMENTS DID COME ALONG.

Figure G6. Annotated drawing of Mercury made by David Graham on the 30th May 2024.

8.3 Images of Mercury

This section contains a selection of images of Mercury obtained telescopically by a number of imagers over a period of nearly 20 years. The images are in chronological order, and what is noticeable about them is the way in which the quality of images has improved, particularly in the last decade. Not surprisingly, images acquired with larger apertures generally show more features on the surface of Mercury, and there has been a trend for amateurs to acquire instruments with larger apertures as they become commercially available. This is no doubt one reason for the improvements in image quality. Another likely reason is the development in planetary cameras that has taken place over the same period. Cameras are now more sensitive, which allows shorter exposure times and reduces the detrimental effects of seeing. Other contributing factors are developments in processing software, greater expertise on the part of imagers and, as mentioned above, the increasing use of instruments with larger aperture. Thanks to these developments, amateur imagers now routinely produce images of Mercury that approach the limits of their equipment and the Earth's atmosphere.

The difficulties of imaging Mercury and processing the data often result in images that have some residual noise, and there may be uncertainty over whether a bright spot is a genuine feature or an artefact of the data or the processing. Imagers deal with this in several different ways, some of which appear in this gallery. One is to present multiple images from different data sets, which is possible if there is enough data. Any features that are present in multiple images are not noise artefacts, because the noise is random, but they might still be generated in the image processing stage. The second approach is to show the image alongside a comparison image obtained from Messenger data, via a source such as *WinJUPOS*, to which a suitable amount of blurring has been applied. This technique is now commonly used. A third technique is to convert images taken on consecutive days into an animated GIF file, so the images are shown alternately, and the common features can be recognised by their slight shifts from one to the other.

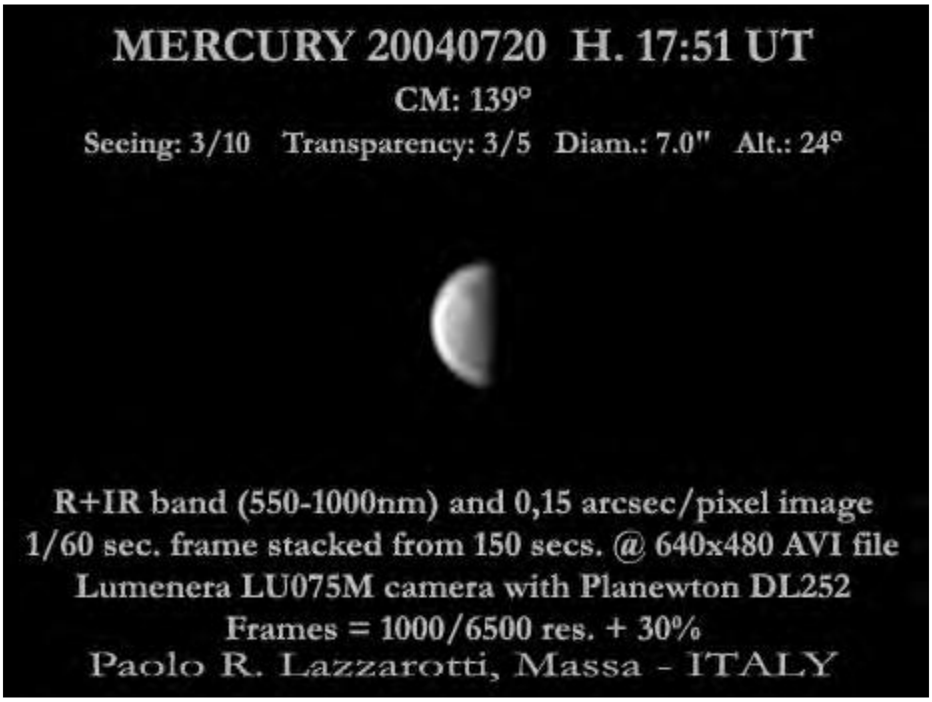

Figure G7. Image of Mercury taken by Paolo Lazzarotti in 2004.

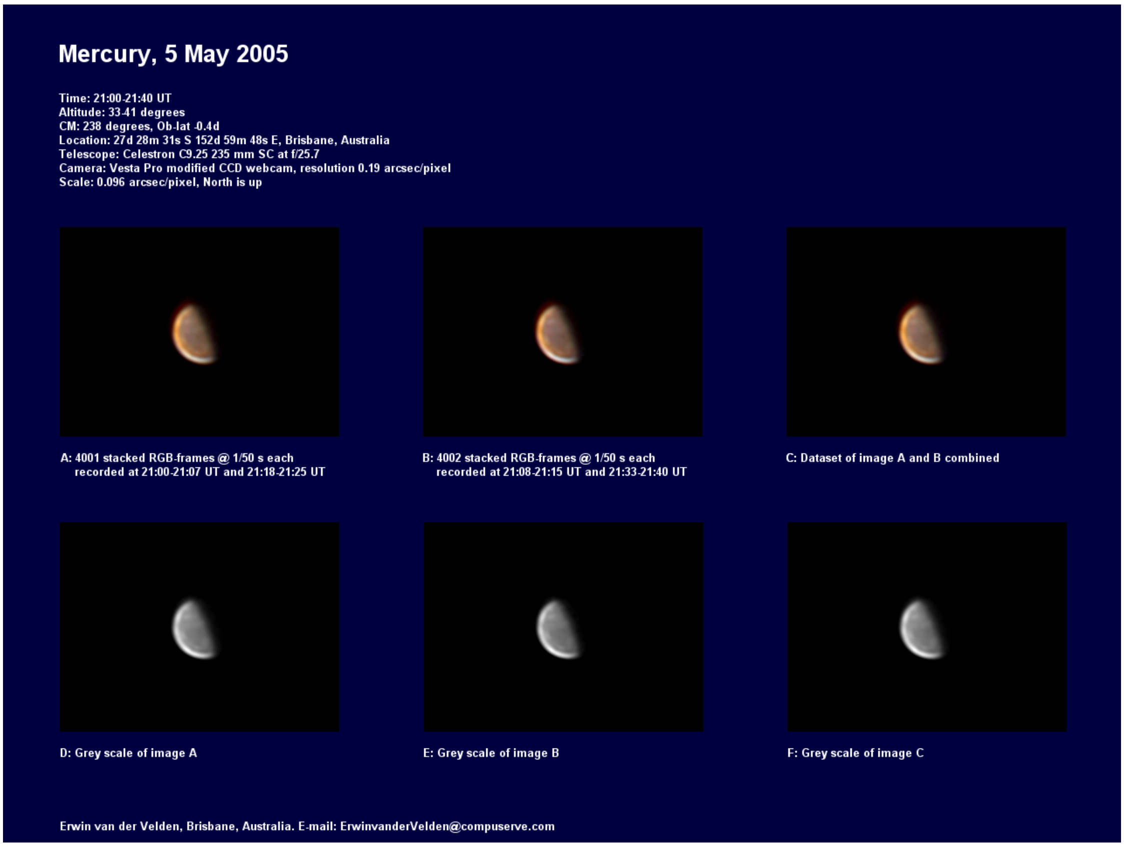

Mercury, 5 May 2005

Time: 21:00-21:40 UT
Altitude: 33-41 degrees
CM: 238 degrees, Ob-lat -0.4d
Location: 27d 28m 31s S 152d 59m 48s E, Brisbane, Australia
Telescope: Celestron C9.25 235 mm SC at f/25.7
Camera: Vesta Pro modified CCD webcam, resolution 0.19 arcsec/pixel
Scale: 0.096 arcsec/pixel, North is up

A: 4001 stacked RGB-frames @ 1/50 s each recorded at 21:00-21:07 UT and 21:18-21:25 UT

B: 4002 stacked RGB-frames @ 1/50 s each recorded at 21:08-21:15 UT and 21:33-21:40 UT

C: Dataset of image A and B combined

D: Grey scale of image A

E: Grey scale of image B

F: Grey scale of image C

Erwin van der Velden, Brisbane, Australia. E-mail: ErwinvanderVelden@compuserve.com

Figure G8. Montage of images from 2005 by Erwin van der Welden.

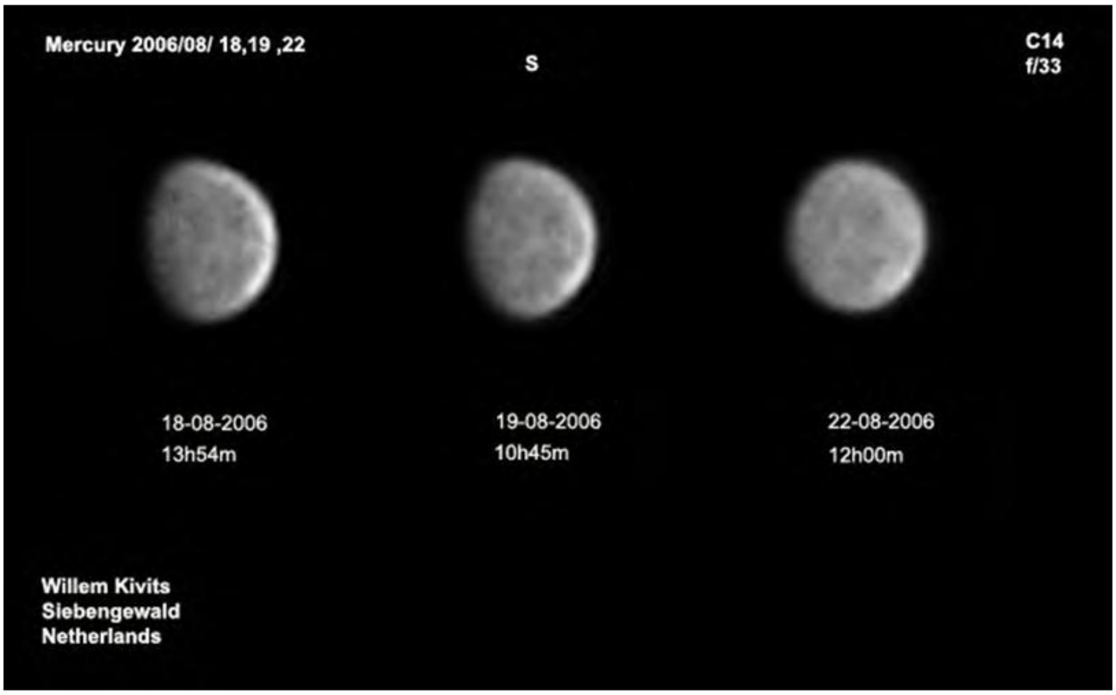

Figure G9. Sequence of images taken by Willem Kivits in 2006.

Figure G10. Image taken by John Boudreau in 2008, compared with Messenger data.

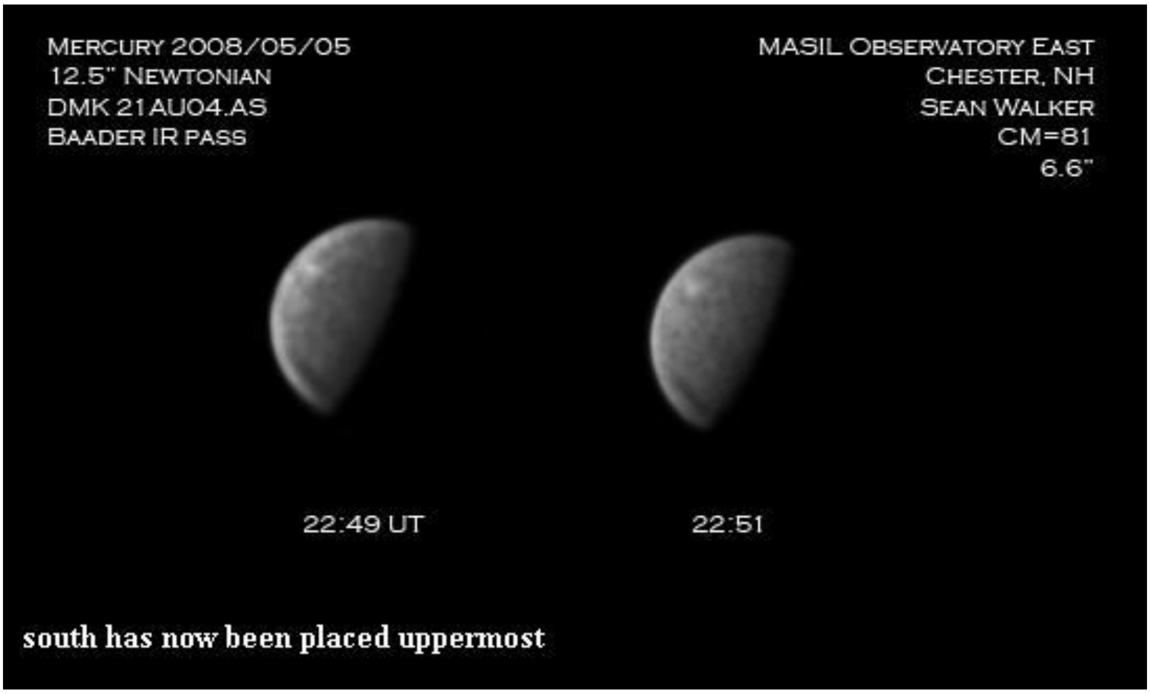

Figure G11. A pair of images captured by Sean Walker in 2008.

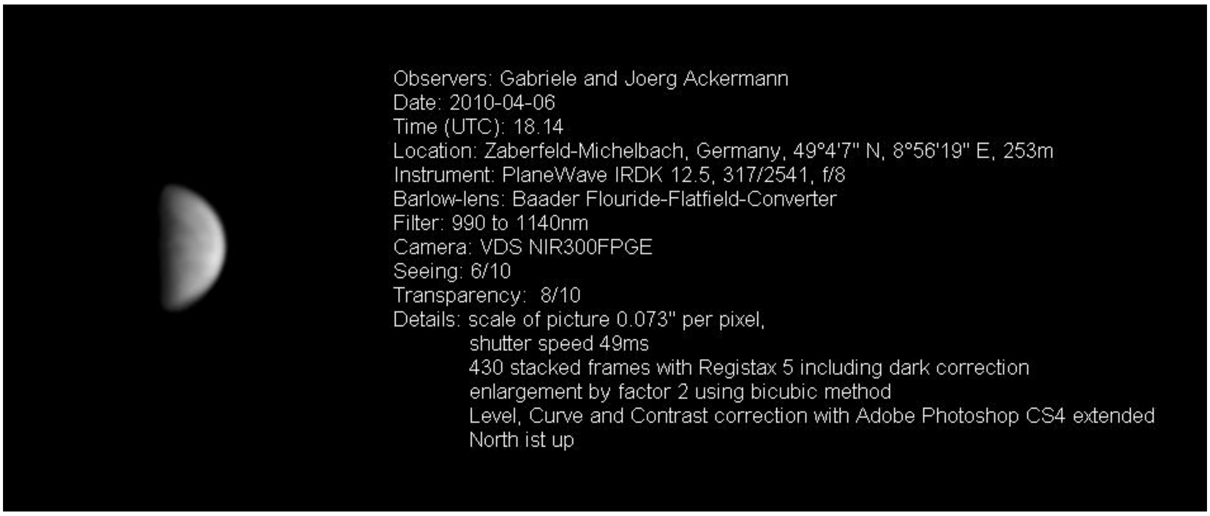

Observers: Gabriele and Joerg Ackermann
Date: 2010-04-06
Time (UTC): 18.14
Location: Zaberfeld-Michelbach, Germany, 49°4'7" N, 8°56'19" E, 253m
Instrument: PlaneWave IRDK 12.5, 317/2541, f/8
Barlow-lens: Baader Flouride-Flatfield-Converter
Filter: 990 to 1140nm
Camera: VDS NIR300FPGE
Seeing: 6/10
Transparency: 8/10
Details: scale of picture 0.073" per pixel,
shutter speed 49ms
430 stacked frames with Registax 5 including dark correction
enlargement by factor 2 using bicubic method
Level, Curve and Contrast correction with Adobe Photoshop CS4 extended
North ist up

Figure G12. An image captured by Gabriele & Joerg Ackermann in 2010.

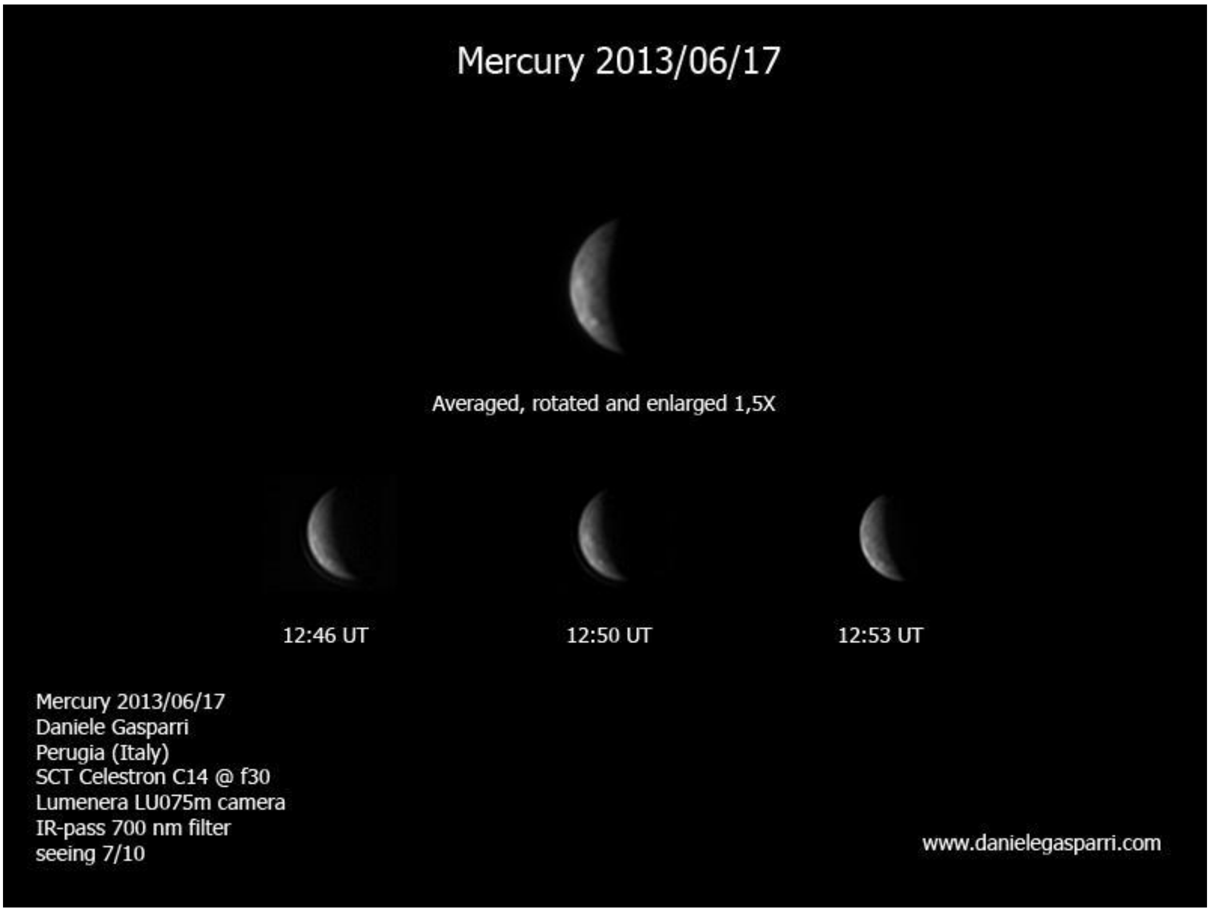

Mercury 2013/06/17

Averaged, rotated and enlarged 1,5X

Mercury 2013/06/17
Daniele Gasparri
Perugia (Italy)
SCT Celestron C14 @ f30
Lumenera LU075m camera
IR-pass 700 nm filter
seeing 7/10

www.danielegasparri.com

Figure G13. Images of a crescent Mercury captured by Daniele Gasparri in 2013.

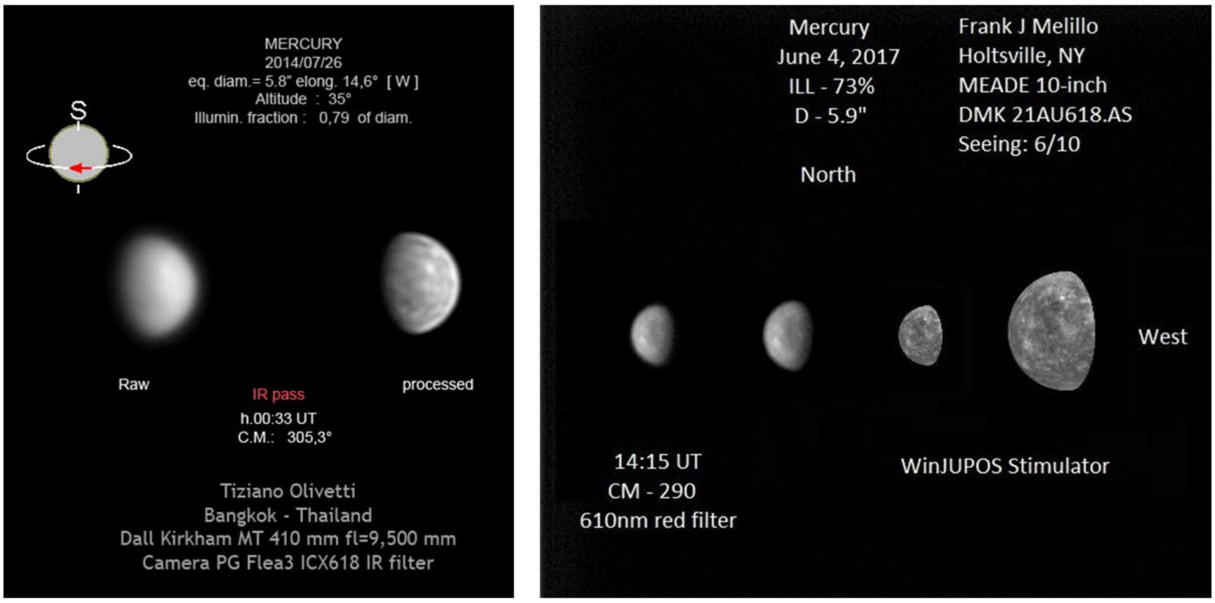

Figure G14. Images taken by Tiziano Olivetti, and by Frank Melillo, with WinJupos comparison.

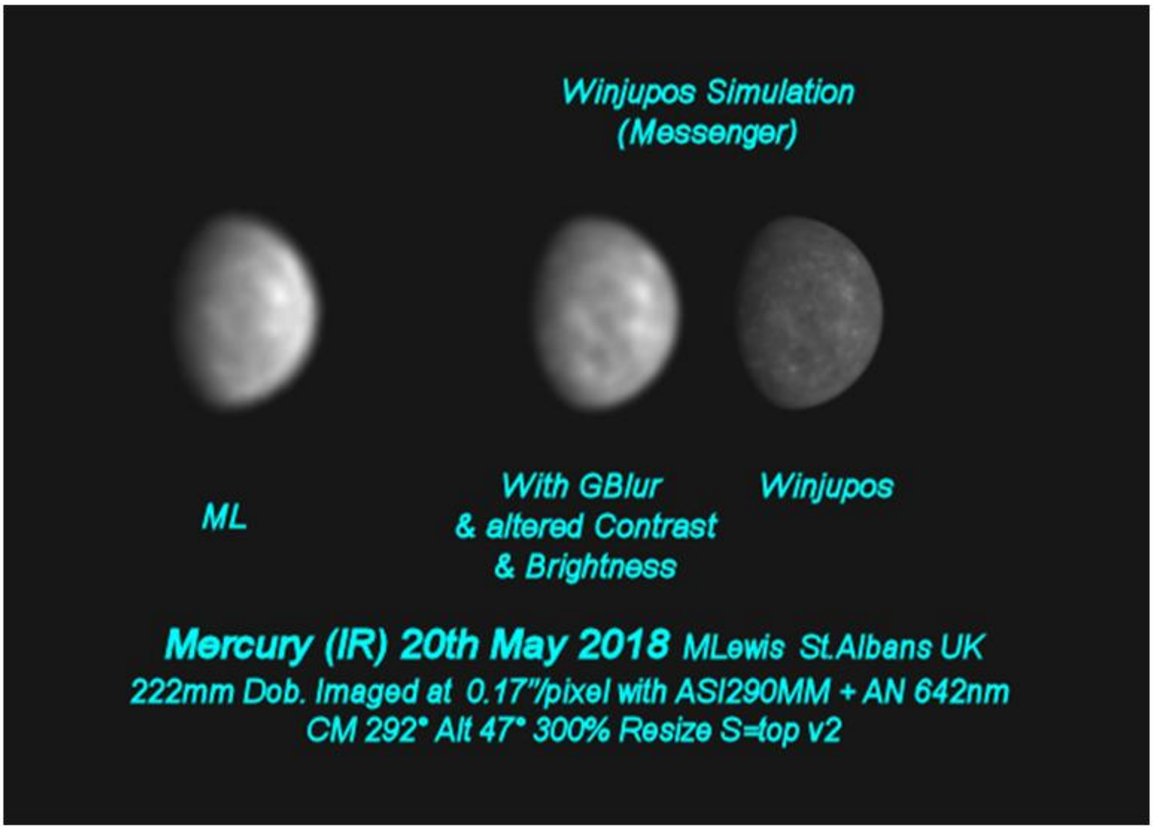

Figure G15. Image taken by Martin Lewis plus comparison with WinJupos.

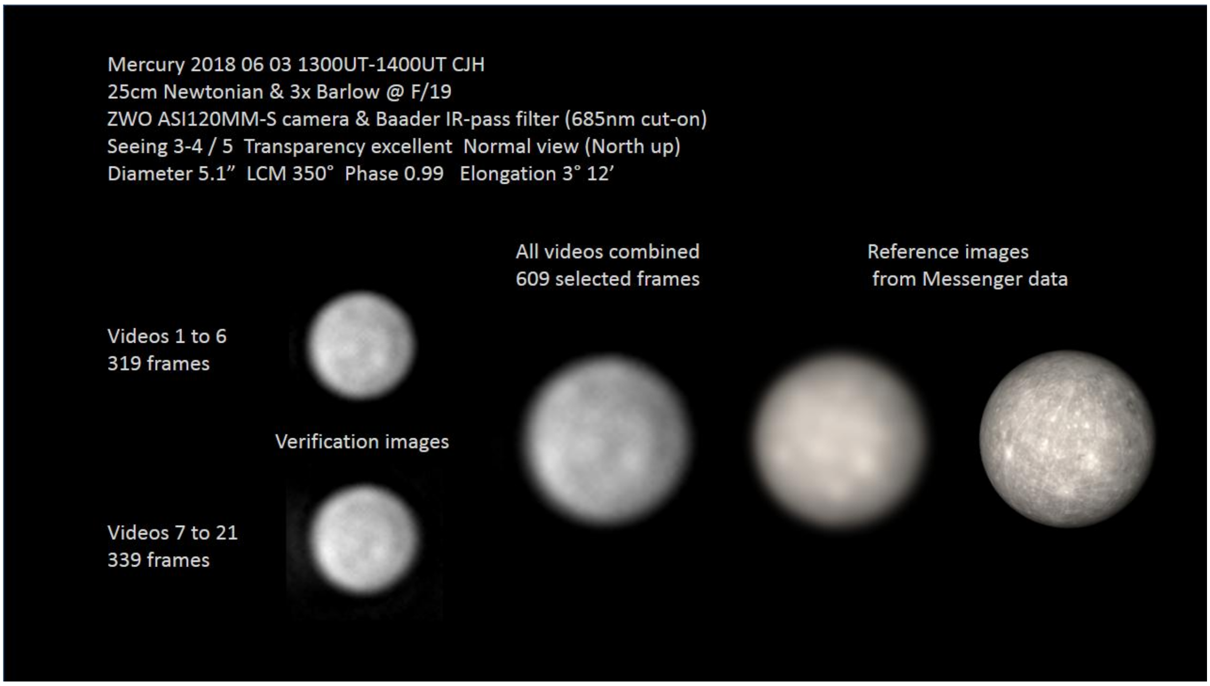

Figure G16. Image of Mercury near superior conjunction (3.2 degrees from the Sun) in June 2018, taken by Chris Hooker using the technique described in Section 7.4.

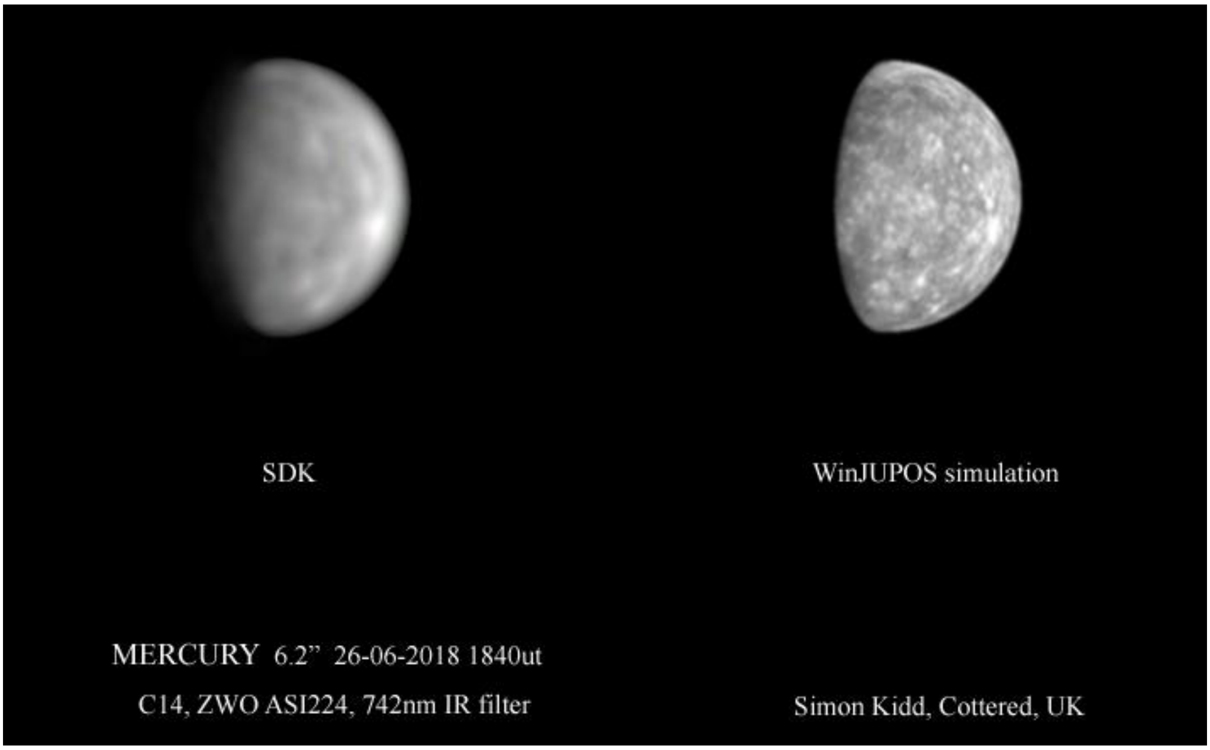

Figure G17. Image of Mercury by Simon Kidd, plus comparison with WinJupos.

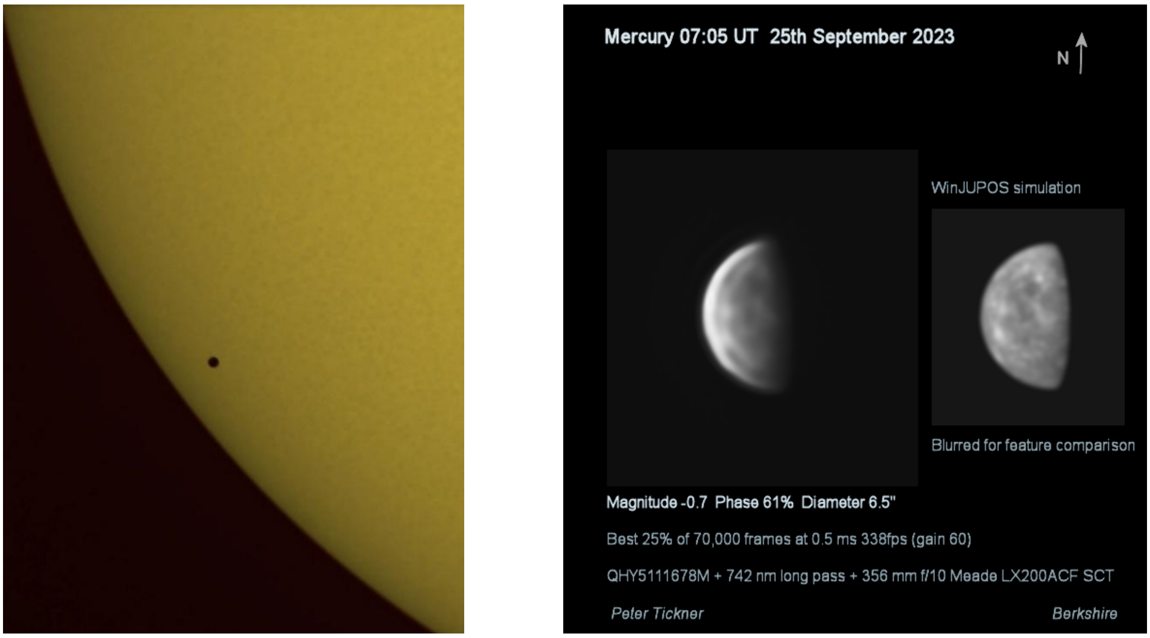

Figure G18. The transit of Mercury on 11th November 2019 taken by Brian Halls (no instrument details available), and an image of Mercury plus comparison with WinJupos by Peter Tickner.

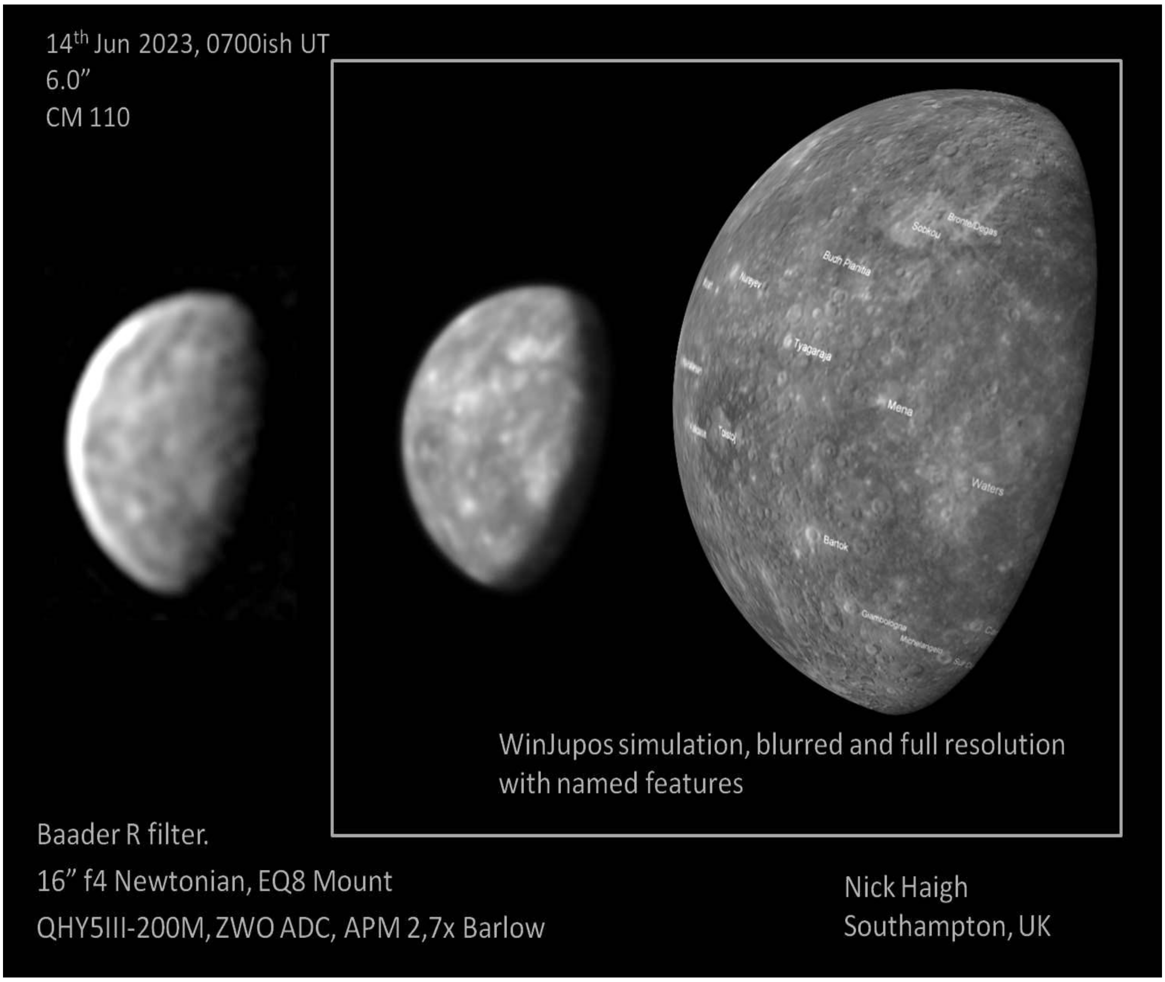

Figure G19. Image of Mercury and comparison with WinJupos by Nick Haigh.

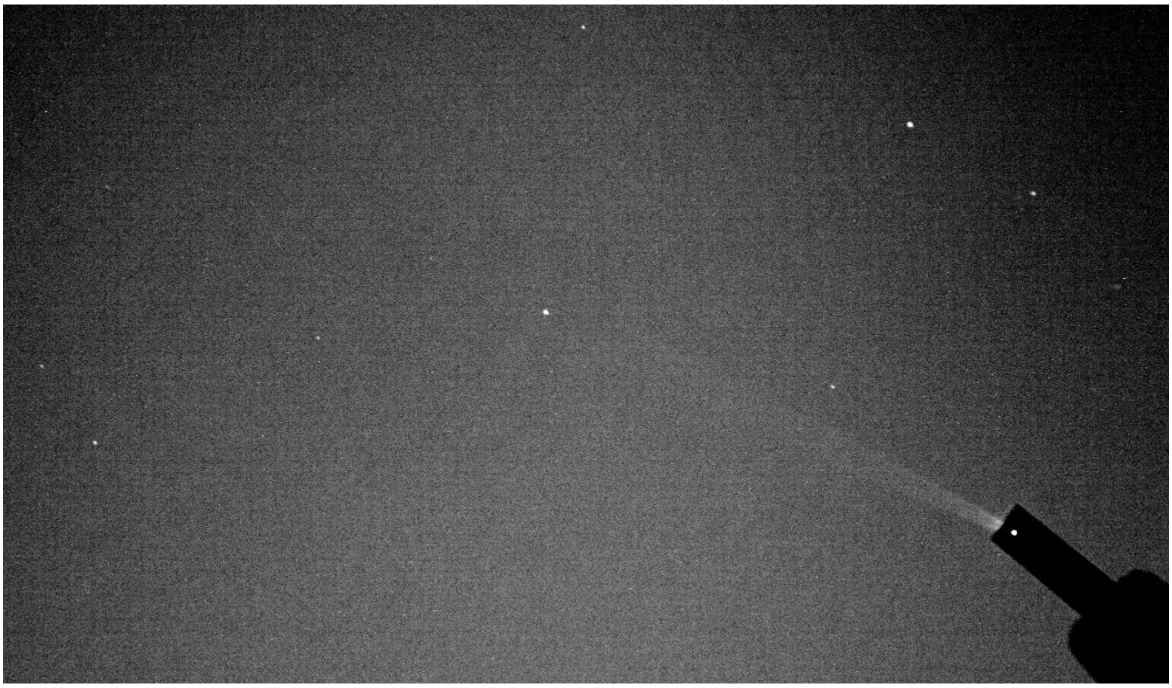

Figure G20. Mercury (lower right behind filter) and its sodium tail imaged with a 589 nm narrowband filter by Chris Hooker on 24th March 2024.

Figure G21. Mercury and its sodium tail imaged without narrowband filtration by Nick James from La Palma on 3rd May 2024.

9. Online resources for Mercury observers

This is a selection of websites and resources the writer has found useful, although it is not intended to be exhaustive. Note that some of the sites listed are not secure, although they and the software listed here are believed to be safe. Visiting any of these sites, and downloading and using any software from them, is entirely at the user's own risk.

British Astronomical Association Mercury & Venus Section:

Main page:	https://britastro.org/section_front/18
Section Reports:	https://britastro.org/node/4937
Notes with Mercury material:	https://britastro.org/journal_old/pdf/118-1notes.pdf https://britastro.org/journal_old/pdf/118-2notes.pdf

Association of Lunar & Planetary Observers [ALPO]:
http://alpo-astronomy.org/index.htm
http://www.alpo-astronomy.org/mercury/merc2.html

Maps of Mercury:
https://history.nasa.gov/SP-423/contents.htm

Messenger website at Johns Hopkins University:
https://messenger.jhuapl.edu/

In-the-Sky.org website run by Dominic Ford:
https://in-the-sky.org/article.php?term=Mercury

Stellarium:
https://stellarium.org/en_CA/

WinJUPOS:
http://jupos.org/gh/download.htm

Image processing software (all freeware):

Registax	http://www.astronomie.be/registax/download.html
Autostakkert!	http://www.astrokraai.nl/software/latest.php
PIPP	https://sites.google.com/site/astropipp/
Iris	http://www.astrosurf.com/buil/iris-software.html
Siril	https://free-astro.org/index.php/Siril

Image processing tutorials and related topics:
https://www.thelondonastronomer.com/#/planets/
http://www.iceinspace.com.au/projects.html
http://planetaryimagingtutorials.com/
http://www.astrofriend.eu/links/links-astronomy-imageprocessing.html

10. Bibliography

E.M. Antoniadi (tr. Patrick Moore), *The Planet Mercury*, K. Reid Ltd, 1974.

Fred W Price, *The Planet Observer's Handbook* 2nd ed., Cambridge University Press, 2000

R.G. Strom and A.L. Sprague, *Exploring Mercury: The Iron Planet*, Praxis, 2003.

Patrick Moore, *Moore on Mercury: The Planet and the Missions*, Springer, 2007.

Gerald North, *Observing the Solar System: The Modern Astronomer's Guide*, Cambridge University Press, 2012.

T.J. Mahoney, *Mercury*, Springer, 2014.

David A. Rothery, *Planet Mercury: From Pale Pink Dot to Dynamic World*, Springer, 2015.

William Sheehan, *Mercury*, Reaktion Press, 2018.

Sean C. Solomon, Larry R. Nittler and Brian J. Anderson (eds), *Mercury: The View after MESSENGER*, Cambridge University Press, 2018.

Acknowledgements

I would like to thank several people who helped enormously with the preparation of this guide. David Gray provided a large part of the information contained in Section 5 on visual observations, and made several valuable suggestions to improve it. Martin Lewis and Simon Kidd reviewed the draft of Section 6 on imaging Mercury, and contributed their own techniques as well as making many insightful and helpful comments. Martin Lewis also read an early draft of the entire guide, made a number of valuable suggestions and spotted several errors. Paul Abel, current Director of the BAA Mercury & Venus Section, reviewed the guide and suggested a number of improvements. The Section's archive of Mercury images was largely compiled by Dr Richard McKim during his time as Director of the Mercury and Venus section, and it also includes scanned copies of paper records of older observations. Thanks to his efforts the archive is a comprehensive and valuable resource, and I am grateful to the Council of the BAA for allowing me to use material from it in Section 8. I thank David Gray and Chris Dole for providing me with photographs to use in some of the Figures. Finally, my thanks are due to Bill Leatherbarrow and the other members of the committee that reviewed the manuscript prior to publication, who recommended some further changes. I am most grateful to all of them for their support and encouragement, but the responsibility for any mistakes that remain is of course mine alone.

Chris Hooker

April 2020

Appendix 1. A parfocal Barlow lens for near-infrared planetary imaging

A1.1 The need for an infra-red Barlow lens for imaging Mercury

There are two main reasons why standard commercial Barlow lenses are not ideal for imaging in the near-IR. In their simplest form, they consist of a single negative achromatic doublet lens with a focal length from -20 to -80 millimetres, designed to have the same focal length at two specific wavelengths. These are usually the Fraunhofer "C" and "F" lines at 656.3 nm and 486.1 nm, and for wavelengths between these lines the variation in focal length is small. Outside the visible spectrum, the focal length changes more rapidly. If imaging is confined to a narrow band of wavelengths the variation of focus will be small, but imagers often use only an IR-pass filter, in which case the long-wavelength limit of the spectrum is set by the sensitivity of the camera sensor, and the chromatic aberration of the Barlow can soften the image significantly. The writer encountered this problem while imaging Mercury using a Baader 685 nm IR-pass filter with a standard 3x Barlow lens. Modern CMOS planetary cameras are sensitive much further into the infra-red than older ones, so this effect will become more noticeable.

The second reason why normal Barlow lenses are less effective for infra-red imaging is that their anti-reflection coatings are designed for visible light and do not perform well in the near-IR, in fact some coatings reflect more infra-red light than an uncoated surface. The result will be greater light loss and brighter internal reflections, reducing the brightness and potentially also the contrast of the image.

Finally, it has been the writer's experience that Barlow lenses are rarely parfocal. In other words, when the Barlow is introduced the telescope must be refocused to obtain a sharp image. At night the defocused image of the target is usually visible, but this is not true when imaging Mercury in daytime. The process of refocusing by a significant amount and then re-acquiring the larger and fainter image becomes far easier if the magnifying system is parfocal with the telescope eyepiece. For all these reasons, therefore, the idea of making a parfocal near-IR Barlow lens was attractive.

A1.2 Design considerations

The small angular size of Mercury led to the choice of magnification of 5x to achieve an image scale of around 0.15 arc seconds per pixel, the writer having previously used a 5x Powermate. The components for the device were bought from ThorLabs. This supplier offers a small range of negative achromatic lenses corrected for 650 nm to 1050 nm in the near-IR. There are four lenses of ½-inch diameter with focal lengths of -20, -25, -30 and -50 mm which all have anti-reflection coatings designed for the wavelength range where the lenses are achromatic. Information on the Thorlabs website showed that the -30 mm and -50 mm lenses both had a maximum focal length at around 750 nm and a variation in focal length of no more than 10 microns between 650 and 850 nm. For comparison, the data for a -30 mm achromat designed for the visible showed a focal length difference of 30 microns just between 650 and 700 nm, a much more rapid change with wavelength.

The spectral region from 650 nm to 850 nm is ideal for imaging Mercury because the surface markings have good contrast and the sensitivity of most planetary cameras is still acceptably high. To limit the wavelength range of the IR Barlow to the region where its focal length variation was a minimum, a short-pass filter was purchased that blocks wavelengths longer than 850 nm. The combination of this and the Baader IR-pass filter transmits a range of wavelengths from 685 nm to 850 nm. The short-pass filter is a dielectric type and therefore relatively expensive, but there are no simple glass filters that have the required short wavelength transmission characteristics. To keep the cost of the device down this filter could be omitted from the initial construction: it can easily be added later if the image still appears to suffer from unacceptable softening due to chromatic aberration.

Calculation of the distances needed to give 5x magnification with the -30 mm lens showed that the primary focus would be 24 mm beyond the lens, and the image distance would be 120 mm. This is acceptable, whereas the -50 mm lens would make the device too long. The writer uses a 254 mm F/6.3 Newtonian for imaging Mercury, and with that focal ratio, the diameter of the focal cone at the lens is 24/6.3 = 3.8 mm. Even after a reduction in aperture due to the lens holder, a lens of ½-inch diameter is large enough to accommodate a primary focal ratio down to F/4.

In addition to optical components, Thorlabs supply a huge range of parts for building optical setups, including threaded tubes of different diameters and lengths to hold optics and filters, and adapters for coupling those tubes to other components. The tubes can screw into one another to build up any required length. Knowing the distances needed for the 5x Barlow, a set of tubes and adapters was purchased at the same time as the lens and filter. A list of the components used to make the device, including Thorlabs part numbers and 2025 prices, is given in a table at the end of this Appendix.

A1.3 Construction of the near-IR Barlow

Tube sections with 1-inch internal diameter (SM1) were used for the main body, as these are robust and easily coupled to the 1¼ inch drawtube adapter supplied with the ZWO ASI174MM camera the writer uses for Mercury. The camera itself has a T-thread fitting, plus an adapter that accepts the standard C-mount thread used on CCTV lenses and also on the 1¼ inch drawtube adapter. The negative achromat is mounted in a section of SM05 tubing (with a ½-inch internal diameter), with its less-curved surface towards the incoming light. The SM05 tube is screwed into a threaded adapter which holds it inside the SM1 tube. This adapter can be moved back and forth along the optical axis, and a position found that makes the Barlow parfocal with a normal eyepiece when used in the telescope. The adapter is then locked in place using a retaining ring from one of the SM1 tube sections. Figure A1.1 shows a cross-section through the assembled device with the main components labelled. Figures A1.2 & A1.3 show the complete device and a partial disassembly in which the different components can be seen. The distance from the shoulder on the drawtube adapter to the front of the camera is 90 mm, which is comparable to many high-magnification Barlow lenses.

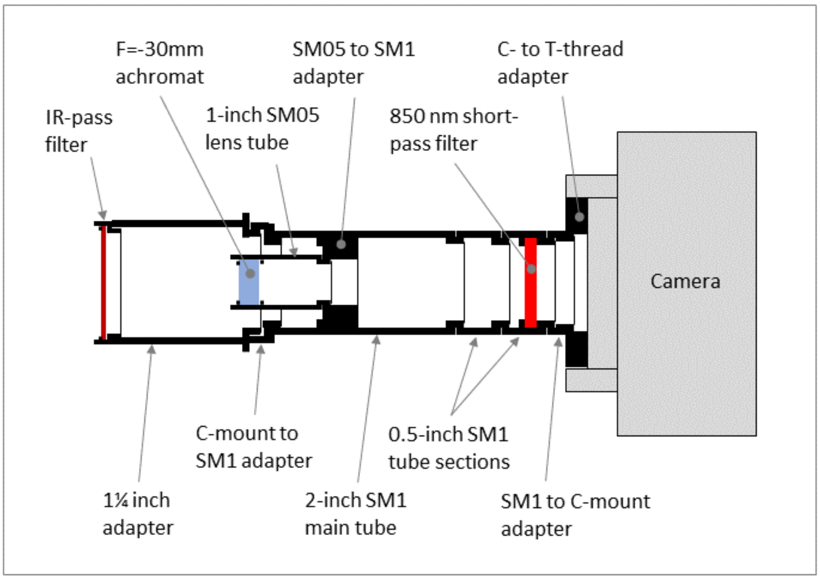

Figure A1.1. Schematic cross-section of the assembled IR Barlow lens.

Figure A1.2. The assembled IR Barlow lens attached to the ASI174MM camera ready for use.

In the disassembled view in Figure A1.3, below, the parts are (from left to right): the Baader IR-pass filter; the 1¼-inch adapter; the C-thread to SM1 adapter; the main SM1 tube section with the SM05 tube holding the negative lens protruding from the end; a ½-inch SM1 spacer tube; another ½-inch SM1 tube carrying the 850 nm short-pass filter; the SM1 to C-thread adapter; the C-thread to T-mount adapter; the ZWO ASI174MM camera.

Figure A1.3. The IR Barlow partially disassembled to show the components. Details in the text.

The Barlow assembly is intended to be attached to the camera and the two used as a unit. To use the camera without the Barlow, the parts can be separated and the 1¼-inch adapter fitted directly into the T-to-C adapter on the front of the camera. To ensure the Barlow assembly can be separated easily from the camera, a spacer ring of 1 mm sheet Teflon (not shown in Figure A2.3) is placed in the recess of the camera body below the C-to-T adapter.

The writer designed this device to have a magnification of 5x. However, the magnification can be changed by, for example, removing the ½-inch tube section before the short-pass filter. The lens can then be repositioned if required, although in practice the image will still be very close to focus after the change. With the -30 mm lens the magnification could be varied down to 2.5x if the correct tube sections were available, although not while the device was in use. To reach 2x or less, the -50 mm lens would work better. Parfocality with an eyepiece could be maintained after any of these changes.

A1.4 Performance tests

After building the device as described, the writer tested it first on a star and then on Mars, which at the time was visible in the west after sunset and had an apparent diameter of only 5.5 arc seconds, similar to Mercury during much of an elongation. The results are shown in Figure A1.4. The image of the star shows a smooth Airy disc and a single faint diffraction ring. The image of Mars shows some detail, though the seeing at the time was poor. During these tests, the position of the negative lens was adjusted slightly to reach the desired parfocal position, in which the visual focus with an eyepiece matched the focus in the infra-red with the Barlow and camera combination.

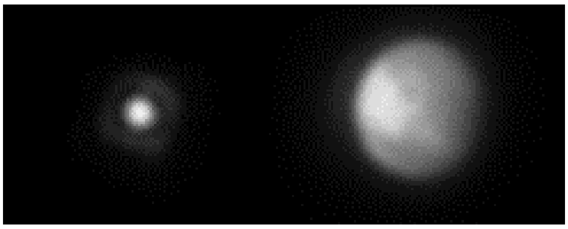

Figure A1.4. Images of a star and Mars with the IR Barlow and a 200 mm Maksutov-Cassegrain

The next time Mercury was suitably placed, the Barlow was tested on it during a daytime imaging session. As expected, the parfocal design made setting up for imaging far easier than with a 5x PowerMate, which required an 18 mm movement of the drawtube to reach focus. On replacing the eyepiece with the Barlow assembly plus camera, Mercury was immediately visible on the monitor, and only very slight refocusing was needed. The image quality with Mercury in daytime is always highly dependent on the seeing, but in good conditions the images obtained showed as much detail as expected. Two examples are presented in Figure A1.5.

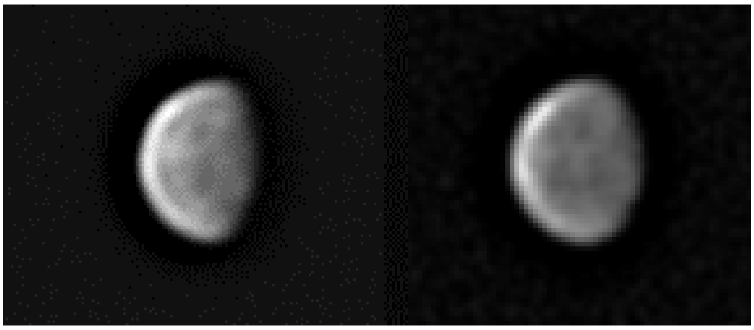

Figure A1.5. Mercury imaged using a 254 mm Newtonian, ZWO ASI174 camera and the writer's 5x IR Barlow. Left: 18th July 2021; right: 5th July

A1.5 Conclusion

The parfocal infra-red Barlow lens described here performs well and has several advantages over conventional Barlows for imaging Mercury or other planets in the near infra-red. The design is flexible and could be changed by the builder to give a different magnification, or even adapted for use in the visible spectrum by selecting a different lens. The writer hopes this design will prove useful to those wishing to image Mercury and other planets in the infra-red and would be happy to advise and assist anyone wishing to build their own version of it.

The following table lists the components used to build the device, with part numbers and 2025 prices.

Table 1. Component list for the IR Barlow lens

Description	**Thorlabs Part No**	**Price £ (2025)**
Adapter with external SM1 & internal C-mount threads	SM1A10	19.06
*SM1 tube section, 2-inch (includes 1 SM1RR ring)	SM1L20	15.28
SM05 tube section, 1-inch (includes 1 SM05RR ring)	SM05L10	13.98
Additional SM05RR retaining ring	SM05RR	3.70
-30mm FL achromat, ½-inch diameter, AR 650-1050 nm	ACN127-030-B	57.72
Adapter with external SM1 & internal SM05 threads	SM1A6T	20.04
*SM1 tubing section, 0.5-inch (includes 1 SM1RR ring)	SM1L05	11.66
SM1 tubing section, 0.5-inch (includes 1 SM1RR ring)	SM1L05	11.66
*25mm dia Premium short-pass filter, cut-off 850 nm	FESH0850	135.41
TOTAL of above items including optional components		**287.91**
**Adapter with external C-mount & internal SM1 threads	SM1A9	18.30
**Adapter with external T-mount & internal SM1 threads	TMA2	22.88

Items marked * are optional depending on the details of the device. If a lower magnification is desired, the 2-inch SM1 tube can be replaced with a shorter one, or the 0.5-inch spacer tube omitted, or both. As mentioned in the text, the relatively expensive short-pass filter could be omitted at first to keep the cost down, and added later if needed to improve the performance of the device.

Items marked ** are alternatives depending on whether the camera to be used has a C-mount thread or a T-mount thread.

The listed prices do not include delivery charges or VAT and are subject to change by the supplier.

Appendix 2: Calculation of angles for imaging Mercury at conjunction.

The important angle to calculate for any given instrument is the minimum angular distance from the Sun at which Mercury can be imaged safely using the technique described in Section 7. Imaging the planet near superior conjunction is only practical with a Newtonian reflector, and the calculation that follows is done for a Newtonian. The relevant distances and angles are shown in Figure A1 below.

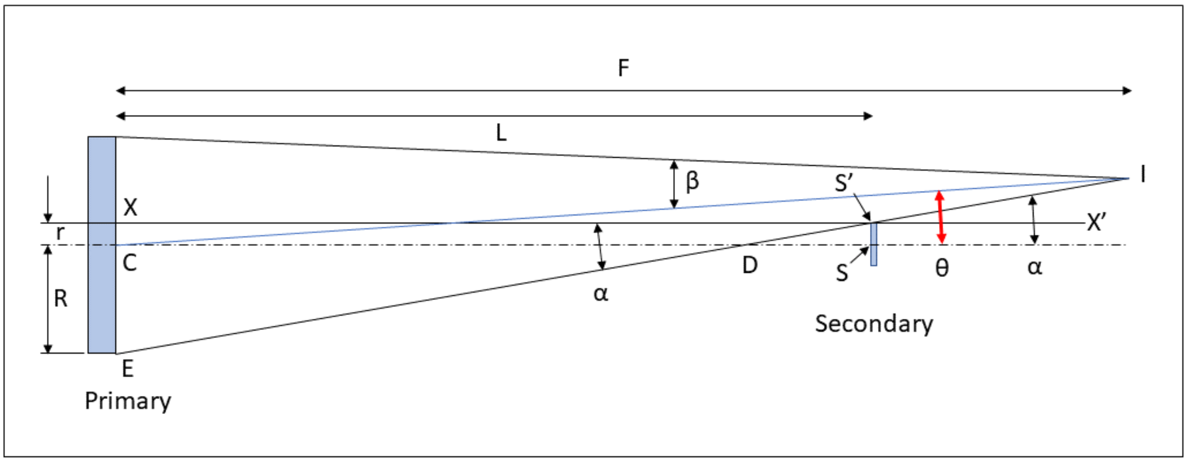

Figure A1. Geometry for calculating the minimum solar distance for imaging Mercury at conjunction.

The telescope has primary and secondary mirrors with radii R and r respectively. The secondary is represented as a disk of radius r at a distance L from the primary, which has a focal length F. The line CS is the optical axis of the telescope, joining the centres of the primary and secondary mirrors. In the initial calculation, the minimum off-axis angle θ is calculated for a point source, the image of which is formed at I by a cone of light converging from the primary. The result is later increased by the angular radius of the Sun to give the required minimum angular separation of Mercury from the Sun.

We need to evaluate the two angles α and β. α is the angle between the optical axis and the extreme ray of the converging cone of light from the primary, shown as EI in the figure, and β is the semi-angle of that cone. The ray EI intercepts the optical axis at D. The angle α between CS and EI is given by

$$\tan \alpha = R/CD , \qquad \text{(A1)}$$

but this cannot be evaluated because we do not know CD. We therefore draw a line XX', parallel to the optical axis, which just touches the edge of the secondary at the point S'. In triangle S'XE the distance XE is the sum of the radii of the mirrors, or (R + r), and the distance XS' is the separation of the primary and secondary mirrors, which is L in the figure. We then have

$$\tan \alpha = (R + r)/L , \text{ or } \alpha = \tan^{-1} ((R + r)/L) \quad . \qquad \text{(A2)}$$

The angle α can now be evaluated provided the dimensions of the mirrors, and their separation, are known. For the writer's telescope R = 125 mm, r = 25 mm and L = 1320 mm, giving a value for α of 6.48 degrees.

The angle β is given to a good enough approximation by the expression

$$\tan \beta = R/F , \text{ or } \beta = \tan^{-1} (R/F) . \qquad \text{(A3)}$$

The writer's telescope has F = 1600 mm, so equation A3 yields a value for β of 4.47 degrees.

In the triangle ICD, the angle ICD is θ and the angle CID is β. The exterior angle of this triangle is IDS, which is equal to α, and by a standard theorem in geometry it is also equal to the sum of the two interior opposite angles. We therefore have

$$\alpha = \theta + \beta \text{ , or } \theta = \alpha - \beta \text{ .} \qquad \text{(A4)}$$

The minimum angular separation of an object from the Sun for safe imaging *if the Sun were a point source* would be, for this telescope, $\theta = \alpha - \beta = 6.48 - 4.47 = 2.01$ degrees. Given that the Sun is not a point source, but has an angular radius of 0.26 degrees, the minimum angle must be increased by this amount, to give a final minimum angle of 2.27 degrees. In practice the writer prefers to leave a safety margin by considering an angle of 2.5 degrees to be the minimum acceptable.

It must be emphasised that this calculation should be used only as a guide to determine when Mercury might be observable near superior conjunction. The observer should always use a card to confirm that no sunlight is hitting the secondary mirror, as described in Section 7.4, and abandon the attempt if that test shows Mercury is too close to the Sun to be observed safety.

The calculation for the maximum distance from the Sun is less critical, but for completeness is given here. The relevant geometry is shown in Figure A2 below.

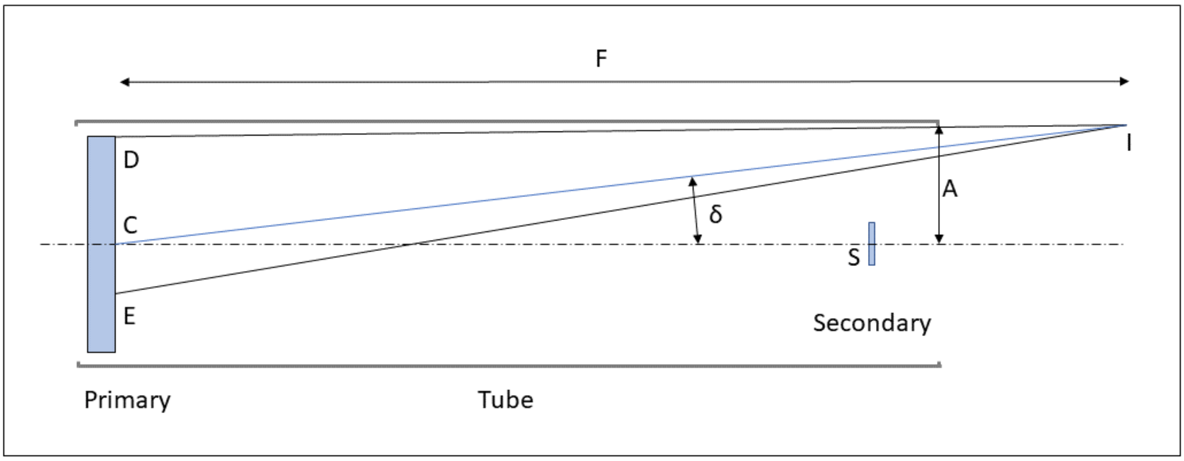

Figure A2. Geometry for calculating the maximum elongation for imaging Mercury at conjunction.

The telescope tube shown in this figure has a radius of A, which will be slightly greater than R. The required angle δ is the angle between Mercury and the centre of the Sun, and also between the axes of the telescope, CS, and the sunlight cone, CI. As before, we first calculate the angle assuming the Sun is a point source. We consider the condition when the extreme ray from the top of the mirror at D just grazes the inside edge of the tube. Because that ray is almost parallel to the side of the tube, the distance of the image I from the axis can also be taken as A. The angle δ is given by

$$\delta = \tan^{-1} (A/F) \text{ .} \qquad \text{(A5)}$$

The writer's telescope has A = 127 mm, which yields a value for δ of 4.54 degrees. To avoid any sunlight striking the inside of the tube, this angle must be reduced by the Sun's angular radius of 0.26 degrees to give a final result of 4.28 degrees. As discussed in Section 7.4, this is not a hard limit like the first one, since a small part of the sunlight cone hitting the tube is not a hazard to the observer, although it may cause heating which could degrade the image.